Physics – Uspekhi **68** (12) 1242 – 1267 (2025)

REVIEWS OF TOPICAL PROBLEMS PACS numbers: **82.39. – k**, **87.10. – e**, **87.50. – a**, 87.50.C –

Radical pair mechanism in magnetobiology: state of the art

V.N. Binhi

DOI: https://doi.org/10.3367/UFNe.2025.09.040032

Contents

Abstract. We discuss the biological effects of weak magnetic fields, a problem that has gone unresolved for nearly half a century. We consider the spin–chemical mechanism of radical pairs, which is prevalent in the literature aiming to explain the observed phenomena. The effectiveness of this mechanism is limited by spin relaxation. The relaxation rate is estimated for a radical in a protein via the Zeeman, hyperfine, spin–orbit, and exchange interactions. Taking the relaxation and chemical kinetics into account, we present an analytic solution of the Liouville–von Neumann equation for two electrons and a nucleus, which relates the magnitude of the effects to the relaxation rate. Various aspects of the solution are discussed: the influence of the radiofrequency and hypomagnetic fields, the role of quantum entanglement, theoretical challenges and prospects, and others.

Keywords: magnetic biological effects, animal magnetic navigation, spin decoherence, spin relaxation, spin chemistry, radical pair mechanism, Liouville–von Neumann equation, open quantum system, chemical compass, hypomagnetic fields

V.N. Binhi
Federal Medical-Biological Agency, Federal Scientific and Clinical Center for Space Medicine and Biology,
Sushchevskii val 24, 127018 Moscow, Russian Federation
E-mail: vnbin@mail.ru

Received 5 October 2024, revised 15 September 2025
Uspekhi Fizicheskikh Nauk **195** (12) 1312 – 1339 (2025)
Translated by S. Alekseev

1. Introduction

As biophysics and molecular biology master nano and subnano ranges of sizes and times, the use of quantum physics becomes inevitable. The study of many biological processes requires a quantum approach [1]. These include photosynthesis [2], respiration, vision, mutations, olfaction, enzymatic reactions in general [3], and, recently, the work of consciousness [4–7]. All these research fields are united under the general name of quantum biology [8–11]. Magnetobiological effects are also quantum. The action of a magnetic field (MF) of the geomagnetic level on organisms is impossible to understand other than as an action on magnetic moments, primarily on the quantum dynamics of electrons.

Extensive literature is devoted to the biological action of weak MFs; reviews are available, e.g., in monographs [12–16]. It is believed that the MF is capable of causing diverse, including toxic, effects in organisms [17]. Chronic exposure to the MF of industrial frequencies with an amplitude of more than 0.3 μT (0.003 G) is recognized by the World Health Organization as a possible carcinogenic factor [18]. At the same time, the average intensity of MF fluctuations on the highways of large cities in the frequency range of 1–100 Hz is about 3 to 4 μT [19]. On the other hand, it has been proposed to use MFs for the treatment of oncological illnesses [20]. The difficulty of assessing the action of an MF on organisms lies in the fact that no convincing physical mechanism is visible that would ensure a noticeable change in the probability of a single act of a chemical reaction in an MF of the order of the geomagnetic field (GMF), about 50 μT. One of the mechanisms relates the biological action of the MF to the presence of magnetic nanoparticles in organisms (see, e.g., [21, 22]). However, many cell cultures and plants reacting to an MF

do not contain magnetic nanoparticles. Therefore, the search for a general molecular mechanism of biological response to MFs continues.

To date, many facts have been gathered about the action of electromagnetic fields on biosystems. The most paradoxical appears to be the action of very small variations in a quasiconstant MF. On the one hand, even the primary molecular target of MF action has not yet been established for such effects. On the other hand, it is clear that the MF can act only on magnetic moments. There are not many types of carriers of magnetic moments in organisms or aqueous systems: they are spin and orbital moments of electrons, protons, and other magnetic nuclei, as well as moments generated by the rotation of multiparticle molecular systems with a nonuniform electric charge density.

In conditions where the primary target of the MF in protein systems is unknown, the main task of theoretical research is to propose a consistent model explaining the effects of weak MFs and allowing experimental verification. The main problem in explaining the effects of weak MFs is the smallness of the magnetic influence on individual microscopic magnetic moments, because they are usually in a thermalized state and their thermal energy kT is 7–8 orders of magnitude greater than the magnetic energy in the GMF.

The apparent paradox of the influence of small MFs $\mu_B H \ll kT$ (where μ_B is the Bohr magneton) was already noted in [23]. There, the influence of an MF on photoprocesses in organic solids was considered, and it was explained by the mixing of spin states of electron–hole-type particle pairs. Even earlier, in [24], it was shown that the result of radical recombination should depend on the MF. From these and subsequent studies, the radical pair mechanism (RPM) [25–28], known in spin chemistry, emerged. It relates the appearance of magnetic quantum effects to practically nonthermalized spin-correlated pairs of electrons. This allows gaining about five orders in the magnitude of magnetic effects compared to simple magnetic spin polarization, and thus explaining the biological action of relatively strong MFs of the order of 10–100 mT or more. However, the observed action of much weaker MFs, at the GMF level and even GMF fluctuations, remains unexplained, which constitutes a problem.

1.1 Radical pair mechanism

The essence of the RPM can be illustrated by the example of the decay of a nonparamagnetic molecule AB into free radicals $\dot{A}$ and $\dot{B}$ with the formation of an intermediate pair of radicals $\dot{A}\dot{B}$, in which transitions $(\dot{A}\dot{B})^S \leftrightarrows (\dot{A}\dot{B})^T$ occur in the spin singlet–triplet states of the pair under the action of the MF:

$$\left.\begin{array}{c} AB \leftrightarrows (\dot{A}\dot{B})^S \\ \downarrow \; \cup \; \uparrow \\ (\dot{A}\dot{B})^T \end{array}\right] \rightarrow \dot{A} + \dot{B}\,.$$

The chemical evolution of the pair depends on its spin state. If the correlated, or coherent, state of spins is long-lived, then the MF also changes the quantity of reaction products by influencing the transition rate. The RPM explains why thermal perturbations do not disrupt the course of the reaction: they do not have time to do so because the magnetic effect develops before the onset of thermal equilibrium. But if spin decoherence is fast, then there is no magnetic effect.

In spin chemistry, various scenarios of the emergence of radical pairs and spin-selective reactions are studied. We are mainly interested in the physical process of decoherence and its influence on the magnitude of magnetic biological effects in the GMF. Therefore, only one of the possible RPM scenarios is considered below, the one relevant to the functioning of organisms.

The idea of the possible involvement of the RPM in the observed response of organisms to MF changes has been known since the early days of spin chemistry as a science [25]. The action of an MF at a level of 5–10 mT on photosynthetic bacteria was explained on the basis of the RPM in [29]: the populations of singlet–triplet states of the pair of photoinduced radicals in the reaction center depend on the MF magnitude, which changes the course of photosynthesis. A year later, it was shown in [30] that, taking the anisotropy of the hyperfine interaction in the RPM into account, one can explain the ability of some biological species to orient in the GMF [31]. This type of RPM with an anisotropic response has been called the quantum chemical compass since then, and is regarded as a prototype of a new type of quantum magnetometer [32–35].

Despite a certain theoretical success of the concept of the chemical compass, the specific molecular target of a weak MF in magnetosensitive organisms remained unclear until 2000. In [36], it was suggested that cryptochrome — a protein participating in many biological processes, for example, in the functioning of the visual apparatus — is responsible for magnetoreception, i.e., the orientation of birds in the GMF. Cryptochromes and related photolyases exist in all organisms and are involved in the work of biological clocks, in the repair of the DNA molecule, in growth processes, etc. [37]. Cryptochromes are found, in particular, in the cones of the retina of the eyes of some birds [38]. Under the action of light quanta from the blue spectral range, a cascade of intramolecular electron transfers between donor–acceptor centers occurs in the cryptochrome molecule with the formation of intermediate pairs of flavin–tryptophan radicals (Fig. 1). Some of them have a quite long lifetime and are apparently magnetosensitive.

The involvement of cryptochromes in magnetoreception, even if not universally [41], has numerous experimental confirmations (see, e.g., [9, 40, 42–44]). Such an assumption agrees qualitatively with experimental facts [45] that (1) magnetosensitivity depends on the spectrum of illumination used, which corresponds to the absorption spectrum of flavin, (2) cryptochromes *in vitro* are sensitive to the MF, although in the range of relatively large MFs of the order of tens to hundreds of mT, (3) cryptochromes are present in the retina of the eyes of some animals and insects reacting to the

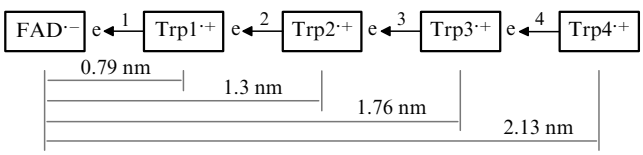

Figure 1. Schematic of electron transport in cryptochrome protein CRY4 (adapted from [39, 40]). Molecular groups of flavin adenine dinucleotide (FAD) and tryptophan amino acid residues (Trp) are transfer centers along electron transport chain. After initial photoexcitation of FAD, four consecutive tunneling events (marked with numbers) generate cascade of FAD–Trp radical pairs. Long-lived FAD–Trp3 and FAD–Trp4 pairs are magnetically sensitive.

MF, (4) these animals do not react to MF reversal, which is a characteristic feature of the quantum mechanical RPM model, and (5) the orientation of cryptochromes in the retina is ordered, which is necessary for the dependence of the averaged magnetic effect on the MF direction. At the same time, it is difficult to quantitatively reconcile the RPM with observations, primarily due to the low sensitivity of the RPM processes to the MF. For brevity, the primary magnetic physico-chemical effect arising via the RPM mechanism is called the RPM effect in what follows. If a number of physico-chemical conditions are satisfied [46], it could underlie the observed response of organisms to a weak MF.

As is known, for the emergence of noticeable primary RPM effects in a weak MF of the order of the GMF, the lifetime of radicals must be greater than or comparable to the precession time of an electron in the GMF, about 0.7 μs. Not all radical pairs arising in photochemical reactions satisfy this condition. For example, experiments in [40] present an *in vitro* analysis of the photochemistry and magnetic sensitivity of recombinant cryptochrome, analogous to cryptochrome in the photoreceptor cells of the eye of migrating robins, known for their magnetoreception. In this protein, in response to photoexcitation, four radical pairs arise that consecutively replace one another (see Fig. 1). Their chemical lifetimes are respectively estimated as 10 ps, 100 ps, 100 ns, and 1–10 μs. This means that only the third and fourth pairs could be magnetosensitive. But a pair lifetime comparable to the electron precession time in the GMF is only one of the necessary conditions for magnetoreception. Besides many biochemical and physiological factors, an important condition is the coherence of singlet–triplet states of the pairs. This requirement entails some problems, as we show below.

1.2 Magnitude of biological effects of weak magnetic fields

The authors of [47, 48] and many others claim that intermediate radical pairs in proteins are sensitive to small MFs of the order of the GMF. However, other studies [45, 49, 50] point to the smallness of the RPM effect and the absence of a reliable explanation for animal magnetic navigation. The discrepancy occurs because there are magnetic effects of different types: those observed in biology, observed in spin chemistry, and calculated theoretically within the RPM framework. They differ in properties, and in magnitude in particular.

The magnitude of magnetic effects observed in biology in low-strength MFs on the GMF level covers a wide range from fractions of a percent to tens and even hundreds of percent [14, 51]. We give just a few examples. Sea turtles in a water-filled arena during seasonal migration were subjected to the MF with slightly, about 10%, changed inclination and module [42]. This forced the turtles to change the direction of movement to the evidently opposite one, which proves the existence of animal magnetic navigation. In [52], the reversal of the direction of a constant MF of about 50 μT led to a decrease in human night vision acuity. The number of errors in recognizing a contrast stimulus increased by 2 to 3 times. In the experiments in [53], a weak static MF influenced the expression of some genes of the plant *A. thaliana*, with well-resolved extrema in magnetic dependences. The measured magnitude could change several-fold and even by an order of magnitude with a change in the MF by 10 μT. In [54], the elimination of the MF promoted the proliferation of neural stem cells from the hippocampus of mice by tens to hundreds of percent. In review [55], several dozen publications are cited where, in response to a 50-μT MF change, a biological response of the order of hundreds of percent was observed.

By contrast, the magnitude of the RPM effects observed in spin chemistry in the GMF is much smaller, not more than 0.01–0.1% (see, e.g., [32, 40, 56, 57]). In [58], the relative magnetic effect in the photosynthetic reaction center of bacteria in the GMF was about 0.3%, which is a uniquely large and unconfirmed value for an RPM process. In [32], the maximum magnitude of the *in vitro* RPM effect was 0.075% for an MF change of 50 μT at liquid nitrogen temperature. In [59], using spectroscopy with pulsed photoexcitation of cryptochrome molecules from the plant *Arabidopsis thaliana*, a 0.05% effect was obtained with the MF variation by a quantity of the order of the GMF. Similar small magnetic effects were obtained in a similar study of photolyase (a protein homologous to cryptochrome) [60]. In *in vitro* studies, the relative RPM effect at 50 μT was 0.025% for flavin–adenine radical pairs [61], and 0.0007% [45] and 0.00003% [62] for flavin–tryptophan radical pairs.

In other words, if we speak about effects in a weak MF of the order of the GMF, then biological effects can be significant, while spin-chemical effects *in vitro* in such an MF usually do not reach even a tenth of a percent. At the same time, theoretical estimates of RPM effects agree well with observations of spin chemistry and do not agree with some biological observations, for example, with magnetic effects in the dark or in the absence of blue lighting [53, 63–66], with sensitivity to the reversal of the MF direction [53, 67, 68], and with the typically large effects observed in a weak MF.

1.3 Fundamental sensitivity limit

The MF starting from which magnetochemical effects acquire a magnitude sufficient for observation is related to the lifetime of the coherent spin state. There is a fundamental relation for the minimally detectable MF H in the Zeeman effect, on which the RPM is based.

The sensitivity of a quantum system to a change in any factor, for example, the MF, is determined by the ability of the system to change by a measurable energy ε during the lifetime of the quantum state τ, i.e., $p \equiv \varepsilon/\tau$. The smaller the value of ε that can be measured, the greater the sensitivity. But due to quantum mechanical principles, ε cannot be arbitrarily small. Consequently, the sensitivity of a quantum system to the MF is limited. The energy–time uncertainty relation [69; 70; 71, p. 202] determines that the measurement of energy ε is possible only with an accuracy of the order of $\hbar/\tau$, where $\hbar$ is the Planck constant. Therefore, we necessarily have $\varepsilon > \hbar/\tau$, which means that $p > \hbar/\tau^2$ [51, p. 152; 72]. To observe a magnetic effect, p must exceed $\hbar/\tau^2$.

By its definition, p is the rate of the process of change in the energy of the system. We speak about the energy of the spin magnetic moment of an electron in a unidirectional alternating MF with the amplitude h and frequency ω. From the expression for moment energies $\pm\mu h \sin(\omega t)$, it follows that the maximum rate of energy change is $\mu h\omega$, whence $\mu h\omega > p > \hbar/\tau^2$. Because $\mu = \gamma\hbar/2$, where γ is the gyromagnetic ratio, by transitivity, we deduce the inequality $\omega\tau > 2/\gamma h\tau$. In a slowly varying MF, i.e., at $\omega\tau < 1$, we obtain the inequality $\gamma h\tau > 2$ as a condition that is necessary for a measurable magnetic effect in an alternating MF with the amplitude h and frequency less than 16 MHz with a realistic lifetime $\tau \sim 10$ ns. Hence, $h \gtrsim 1$ mT.

In the case of a spin magnetic moment in a precessing MF — in constant and perpendicular alternating MFs H and $h\sin(\omega t)$ — the moment energy varies with the Rabi frequency Ω, where $\Omega^2 = (\gamma H + \omega)^2 + (\gamma h)^2$, as $\mu H \gamma^2 h^2 \sin^2(\Omega t/2)/\Omega^2$ (see, e.g., [14, p. 371]). Let $H = h$ for estimation, and the MF frequency ω correspond to the low-frequency range, i.e., $\omega \ll \gamma h$ (8.8 MHz in the GMF). Then, $\Omega \sim \sqrt{2}\gamma h$, and the maximum rate of change of the magnetic moment energy is $\sqrt{2}\hbar\gamma^2 h^2/8$. This gives the inequality $\gamma^2 h^2 \tau^2 > \sqrt{32}$, i.e., practically the same value of $\gamma h\tau$ as in an alternating unidirectional MF. The precessional dynamics of an abstract magnetic moment depends on the product $\gamma H\tau$ [73], which gives approximately the same inequality.

We can arrive at a similar relation for constant MFs using another reasoning. According to the energy–time uncertainty relation, the lifetime of a quasistationary quantum state is related to the spread of the experimentally determined energy of the state, $1/\tau \propto \Delta\varepsilon$, i.e., to the width of the level. On the other hand, energy sublevels of the magnetic moment become degenerate, or mixed, when their width is comparable to the Zeeman splitting caused by the applied MF H. The width of sublevels is of the order of $\hbar/\tau$, and the splitting is $\hbar\gamma H$. Then, there is a critical, or threshold, MF determined by the approximate equality of these quantities, or by the relation

$$\gamma H\tau \sim 1\,. \tag{1}$$

Upon reaching such an MF, qualitative changes at the quantum level must occur. A simple understanding of this condition is that a reliable registration of the change in the moment energy with a change in the MF is possible if the energy change μH is greater than the measurement uncertainty $\hbar/\tau$, i.e., if $\gamma H\tau \gtrsim 2$. In the vector classical model of spin, a magnetic effect is visible if the precession rate of the moment γH exceeds the decoherence rate $1/\tau$, which again gives (1). This general and universal condition links the MF in which a noticeable biological effect could be observed with the microscopic characteristics of the target and its environment — γ and τ. In what follows, we clarify how this necessary condition can be satisfied in the RPM. It is surprising that the relation that is most important for magnetobiology has such a simple form and is related to one of the deepest quantum mechanical principles [70].

According to (1), to explain biological effects induced by MF changes of the order of the GMF, 5–50 μT, the lifetime τ must exceed 0.1–1 μs. It is not yet clear whether radicals, so well isolated from thermal perturbations of the medium and responsible for magnetic effects, can appear in proteins at physiological temperature. The problem becomes especially acute when discussing biological effects of geomagnetic variations, which are another 100 to 1000 times smaller than the GMF. This would now require millisecond decoherence times.

1.4 Relaxation and decoherence

In quantum mechanics, *decoherence* means the evolution of the state of a quantum system from pure to mixed due to interaction with a thermostat [74]. In this paper, the term decoherence is used in the direct sense: it is the loss of coherence of an initially coherent spin state, not necessarily due to interaction with a thermostat. Variation in the MF magnitude (but not direction) changes the phase of the spin state without changing the energy. If such variations are random, the spin state loses coherence. The term *decoherence time* reflects this situation: there is no relaxation here yet, but only a phase mismatch.

The equation for spin dynamics in the RPM for a pair of electrons in the MF is the Liouville–von Neumann equation with chemical kinetics and usually a pure initial state. The quantity of the chemical reaction product at the end of evolution in such a scenario depends on the MF. But if the initial state is not pure (is completely mixed), then no magnetic effect arises. If a pair of spins, starting from a pure state, evolves in the MF while simultaneously losing mutual coherence, then the magnetic effect decreases accordingly. Therefore, spin decoherence in the RPM is a process that exerts a decisive influence on the magnetic effect. To account for it, a term describing the relaxation of the density matrix to an equilibrium completely mixed state with a characteristic relaxation time is added to the equation of spin dynamics. As we show in what follows, there are reasons to assume that the spin decoherence and relaxation times coincide in weak MFs.

With the increase in the MF, spin relaxation separates into two well-distinguishable processes with their own characteristic times. How does the spin decoherence time τ in the RPM relate to spin relaxation times T_1 and T_2 in the phenomenological Bloch equations? These describe the dynamics of the magnetic moment of a uniform ensemble of spins in the MF, in particular, the resonant absorption of energy of an additional alternating MF — the electron paramagnetic resonance (EPR). If the magnetic moment is initially polarized in the direction of the MF, then T_1 and T_2 are the respective time scales of relaxation of the moment projections along and across the MF, due to the interaction of spins with the environment and with each other (see, e.g., [75, p. 360]). In other words, these are times of longitudinal and phase relaxation. Here, the phase relaxation time is, in its very essence, the decoherence time. The interaction of spins with the thermostat not only acts towards the equalization of level populations with a characteristic time T_1 but also contributes to the destruction of spin coherence, and therefore $T_2 \leqslant T_1$ [24; 76, p. 211]. The times $T_{1,2}$, like the Bloch equations themselves, give only an idealized description of relaxation. The influence of various physical factors of a real situation on relaxation and the shape of EPR spectra is discussed, e.g., in [77, 78]. Solutions of the Bloch equations show that the width of EPR lines in small alternating fields is proportional to $1/T_2$.

The field of hyperfine interaction (HFI) — the magnetic coupling of an electron to the nucleus — is a natural atomic scale of the MF. The GMF is an order or two smaller than the most common values of the HFI MF. That is, from the spin dynamics standpoint, the GMF is a zero MF. In a zero MF, there is no preferred direction, and the concepts of T_1 and T_2 become meaningless. However, the concepts of decoherence and relaxation of spin coherence preserve their meaning: the time T_2 becomes the decoherence time. We note that the lifetime of the quantum state of a single spin τ in (1) and the decoherence time in a weak MF have the same relation to the experimentally measured linewidth. Therefore, in relation to a single spin, these times are identified. But, in the RPM in a weak MF, the coherence relaxation time is half that for a single spin, because we are speaking about the mutual coherence of a pair of spins influencing the magnetic effect. The notation τ is also used in what follows for this time, which does not cause confusion. Moreover, a characteristic rate of chemical reaction also appears in the RPM: it determines the

lifetime of spins in the RPM, which therefore differs from their decoherence time.

In EPR spectroscopy, a several-fold decrease in T_2 does not lead to the disappearance of the absorption line; it can only proportionally increase its width. In the RPM, such a decrease in the decoherence time can, as is to become clear from the discussion below, completely suppresses the magnetic effect. For the RPM, spin coherence is of decisive importance: in its absence, magnetic effects simply do not arise. Even if the characteristic time of population equalization of different-energy quantum levels is large, which is detectable by spectral methods (see, e.g., [59, 60, 79]), the spin decoherence time can be much shorter [80, p. 51], which leads to the impossibility of observing RPM effects. Actually, the question of the spin coherence relaxation time — of the decoherence time of radical pairs in proteins — is central to explaining the biological action of weak MFs.

Below, we show that (a) the magnitude of RPM effects, where they are real in the GMF, is proportional to τ^3, and hence drops rapidly with a decrease in τ, and (b) there are grounds to believe that the decoherence time of electron spins in magnetosensitive proteins at a physiological temperature is less than two to three ten nanoseconds. Therefore, the magnitude of the RPM effect in proteins is not more than 0.01–0.1% at 50 μT, a value that also follows from (1). If the characteristic time τ_{ch} of the chemical process is noticeably less than τ, then it follows that $\gamma H\tau_{ch} \sim 1$, and the magnetic effect is all the more indistinguishable. Thus, due to cubic nonlinearity, the question of spin decoherence time is equivalent to the question of the observability of the RPM effect. By changing τ in calculations by just several times, we can effectively switch the magnetic effect on or off.

At realistic decoherence times, the calculated magnitudes of the RPM effects are small and, like the spin chemistry data, do not correspond to magnetic effects observed in biological experiments. Nevertheless, the RPM has long been regarded as a basis for explaining both specific magnetoreception and nonspecific (without special receptors) biological effects of the GMF [13, 81–85], which is achieved by introducing a controversial *ad hoc* assumption into the theory that spin decoherence is slow compared with the characteristic time τ_{ch} of radical chemical kinetics. This allowed not taking decoherence into account at all [30, 33, 36, 50, 86–99], which facilitated analytic studies and agreement with experiment. If decoherence was taken into account, it was assumed that $\tau > \tau_{ch}$, an order of magnitude greater than 1 μs in [88, 100] and many other studies, and even up to 1 ms in [101, 102], which is practically equivalent to the absence of decoherence.

1.5 Experimental data on spin decoherence time

Studies of spin relaxation are traditional for the field of magnetic resonance [103]. Spin relaxation of electrons is well investigated in solids and liquids in [78, 104–108] and in many other studies, but noticeably less in proteins [109, 110]. The experimental study of radical intermediates in proteins is hindered by their low concentration, low availability, and short lifetime.

What is known about the spin decoherence time of magnetosensitive pairs of radicals in proteins? Unlike measurements of the time T_1, which, as a reflection of quantum level populations, can be seen directly from the results of time-resolved EPR spectroscopy, data on T_2 are scarce. There is indirect information from experiments, analytic calculations, and numerical simulations. This implies a large scatter of possible values (by orders of magnitude) and a strong dependence on the properties of the radical, the environment, and other factors.

The relaxation times $T_{1,2}$ of organic radicals in nonviscous liquids at physiological temperatures are relatively large, of the order of 1 μs. This is explained by rotational diffusion of radicals, which averages anisotropic interactions and effectively suppresses spin relaxation [111, p. 117]. The decoherence rate of nitroxyl radicals, for example, is also influenced by various vibrational modes [112]. In viscous liquids and solids, $T_2 \ll T_1$ [24]. For spin tags at a physiological temperature in biological systems, T_2 is usually approximately an order of magnitude less than T_1 [113]. It is shown in [114] that the relaxation time T_2 of nitroxide radicals in liquid decreases with increasing liquid viscosity due to the deceleration of diffusion rotations; in a 70% aqueous solution of glycerol, T_2 was about 200 ns. In [115], T_2 of stable radicals in an *l*-alanine crystal at room temperature was measured by the spin echo method to be 240 ns, which is explained by rapid rotations of methyl groups. The nitroxide radical in aqueous solution was investigated in [116] by various EPR methods; the time T_2 was 50–200 ns. For many ion-radicals of cycloalkanes in nonpolar solvents, this time is 5–20 ns [28, 117]. Heteroorganic oxygen radicals can relax even in 1 ns [118]. Fast relaxation of this radical and others with increased symmetry is explained by the accidental degeneracy of the ground electron state and the resulting strong spin–orbit coupling [119].

In general, the slow spin relaxation of radicals in liquids is related to fast rotational diffusion. It is absent in short-term intermediate pairs of radicals in protein globules, which are tightly folded amino acid chains. Unlike radicals in liquid, radicals, for example, in the reaction center of an enzyme are surrounded by close neighbors and have only limited rotational vibrations. There, we can expect substantially shorter times, or higher rates, of spin relaxation [27, p. 117].

EPR spectra are obtained in many cases by varying the constant component of the modulated MF at a fixed frequency and amplitude h of the radiofrequency (RF) magnetic field. The width L of the resonance line expressed in MF units then satisfies the relation $L^2 = 1/(\gamma T_2)^2 + h^2 T_1/T_2$ [116]. At small amplitudes, $L \approx 1/\gamma T_2$, which is convenient for estimating T_2. However, the absorption signal in this case is also small. The absorption signal grows upon increasing the amplitude, but the width of the resonance line also grows, and hence the resolution of the spectrometer decreases. Compromise values of the RF field power are chosen from which it is difficult to evaluate h [120]. Therefore, it is practically impossible to estimate T_2 from the linewidth of known EPR spectra of intermediate radicals in proteins without knowing the dependence $L(h)$. But the results of measurements of T_2 of such radicals by other methods, for example, by the most suitable spin echo method or the saturation method from the curve $L(h)$ [104], are clearly insufficient for reliable generalizations.

Works on EPR spectra of intermediate organic radicals and spin probes in proteins (see, e.g., [121–129]) typically demonstrate spectra with linewidths of the order of 0.2–5 mT. Review [130] presents general results of the study of intermediate radicals of flavoproteins by EPR methods and continuous and pulsed electron–nucleus double resonance. The width of the EPR signal of anionic and neutral forms of the flavin radical was 1.2–2 mT. In general, such data could correspond to a phase relaxation time in the range of about 1–

25 ns at low power of the RF field and in the absence of factors of inhomogeneous broadening, but this is usually not the case. The time T_2 of quinone radicals arising in the process of photosynthesis was measured using pulsed EPR in a very strong MF, 3.4 T, at a temperature of 120–190 K, and was explained by thermal fluctuations of the g-factor [131]; the shortest time was about 600 ns.

Technical limitations on the formation of high-frequency pulses for spin echo do not allow measuring T_2 shorter than approximately 50 ns. The EPR method of fast scanning of microwave field frequency without pulse formation makes it possible to lower the limit by an order of magnitude [132, 133]. However, so far, there have been no measurements of this type of T_2 of radicals that could form the basis of nonspecific magnetic effects.

In [59], based on theoretical data on exchange interaction in radical pairs [134], the decoherence time in the FAD–Trp pair, separated by a distance of 1.32 nm, was estimated at 10 ps. Indirect data on the spin decoherence time of radicals appearing in active sites of enzymes are related to the magnitude of the MF causing a noticeable response in reactivity. For example, in horseradish peroxidase [135] and DNA polymerase [57], an RP intermediate is involved in the chemical process in the active site. Its spin decoherence time in accordance with (1) is presumably small, less than 1 ns, judging by the fact that a magnetic effect of a 1% magnitude appears in an MF greater than 10 mT.

In biochemical systems *in vitro*, a suitable experimental procedure for finding τ is the method of quantum beats, which is much more sensitive than EPR, because it relies on photon counting rather than on energy absorption [28], and on spin echo methods. Similar studies regarding radicals of interest for magnetobiology are apparently lacking. Thus, so far, there are no experiments testifying to the existence of long spin decoherence times, exceeding 1 μs, in intermediate radical pairs in proteins at room temperature. The *in vitro* experience in spin chemistry, in good agreement with theoretical estimates, limits τ to less than 10 ns and, possibly, to 100 ns in some exceptional cases. However, to observe noticeable RPM effects, this time must be of the order of τ_{ch} or greater. It is clear that relation (1) also imposes a limitation on τ_{ch}, which in estimates is usually taken equal to 1 μs or more [40, 49, 88, 91, 136, 137]. Therefore, many theoretical studies have been aimed at substantiating or searching for conditions under which $\tau \gtrsim \tau_{ch} \sim 1$ μs.

1.6 Calculation data on decoherence time

In view of the uncertainty of the experimental values of the decoherence time of radical intermediates in presumably magnetosensitive proteins, τ was estimated based on the correspondence of magnetic effect magnitudes in experiments with numerical solutions of the RPM equations, where τ was used as a model parameter. Correspondence within an order of magnitude gave grounds to assume that the values of τ used are close to the real ones. This approach is methodologically questionable, because the magnitudes of magnetic effects, both in experiment and in calculations, depend on a multitude of conditions. Nevertheless, it allows obtaining at least a rough idea of possible decoherence times or an idea of the imperfection of RPM models, when the calculated electron spin decoherence times turn out to be implausibly large, of the order of 1 ms.

In [81], magnetic effects in the radical system of coenzyme B12 were theoretically calculated, reaching 10% in the MF of the GMF level with a large chemical lifetime of 50 μs for pair radicals, but without taking thermal relaxation into account, i.e., assuming that $\tau > 50$ μs. At the same time, the authors quote arguments in favor of the fact that, in organic radicals in quasi-solid-state conditions, as in enzyme proteins, the spin relaxation time could reach 1 μs. But no experimental confirmations have appeared in the nearly 30 years since then.

In the calculations in [49], the relative RPM effect in the simplest configuration of 'two electrons, one proton' also amounted to about 10% with a variation in the MF by the GMF magnitude. The problem here is that an unlikely time of 1 μs for thermal relaxation of pair electrons in a biological environment at the physiological temperature was used for calculations. This spin relaxation time is characteristic of organic radicals with fast rotational diffusion in nonviscous liquids [27, p. 117]. In a solid with a low-symmetry environment of the radical, this value is theoretically unsubstantiated.

In [101], the Liouville–von Neumann RPM equation with a Lindblad dissipator was solved numerically, but without chemical kinetics in a constant–alternating MF corresponding to the magnetic resonance condition. The solution could be made consistent with experimental observations if a decoherence time of no less than 100 μs was used in calculations. On this basis, the authors concluded that the decoherence time of spin states of the chemical compass in birds is indeed greater than 100 μs.

Another modification of the method of estimating τ by comparing theory and experiment consists in numerical simulation of random perturbations that cause decoherence. Modulation of the dipole interaction of spins of radicals experiencing translational diffusion in micelles was studied by the Monte Carlo method in [138]. The micelle radius was varied starting from 1.5 nm, which approximately corresponds to the separation of tryptophan radicals in proteins. The rate of relaxational mixing of singlet–triplet states of a photochemically initiated radical pair in the MF ranging from 0.1 to 1 mT due to diffusion was 5×10^7 s^{-1}. Here, the decoherence time could be about 20 ns.

In [139], to study the role of spin relaxation, a cryptochrome molecule with a known molecular structure — a protein of the magnetosensitive plant *Arabidopsis thaliana* — was chosen as a model. In this molecule, flavin–tryptophan radical pairs form under the action of photoexcitation. Thermal perturbations of the radical geometry affect the spin relaxation time due to modulation of the anisotropic HFI. Redfield's theory allows estimating decoherence time from the properties of the stochastic dynamics of the environment and the form of the interaction operators. Estimates of stochastic dynamics were carried out by computer simulation of thermal rotational librations of radical parts. The decoherence time was estimated to be in the range of 76–330 ns. The authors of [139, 140] believe that spin relaxation occurs due to HFI modulation, and do not include other relaxation channels that could give coherence loss rates orders of magnitude higher. Besides, estimates of τ based on the HFI of tryptophan radicals with the nearest-nuclei moments do not take into account that spin decoherence in the RPM is due to not only tryptophan radicals but also the flavin radical, whose spin decoherence can occur faster [124].

Thus, the decoherence times used in estimates of RPM effects of a significant magnitude, i.e., agreeing with experiment, were ~ 1 μs in [49, 100, 136, 139], ~ 10 μs in [137],

~ 100 μs in [101], and ~ 1000 μs in [102]. Some studies where decoherence was not taken into account at all, i.e., it was assumed $\tau = \infty$, are cited above.

Thermal perturbations of the medium transform into fluctuations of the equivalent local MF on a spin via modulation of different interactions. Spin relaxation of paramagnetic centers is generally caused by random modulation of hyperfine, spin–rotation, spin–orbit, exchange, dipole–dipole, and Zeeman interactions, as well as by kinetic processes. Direct theoretical calculations of the decoherence time via channels of one of these interactions or another have been undertaken.

Spin decoherence time is usually associated with T_2, and this term itself requires that the theoretical models satisfy conditions under which it is meaningful, i.e., the MF is nonzero. Therefore, calculations of T_2 are usually carried out within theories where Zeeman interaction is included in the spin Hamiltonian [75, 104, 141, 142].

In substances allowing a description of sound vibrations with the help of phonons, various spin relaxation mechanisms based on spin–phonon interaction have been considered (see review [143]); here, the time T_1 was calculated using the EPR linewidth in a not very small alternating MF as a model parameter, and hence estimates of T_2 remained outside the scope of calculations. For studying spin relaxation in crystals, a complex diagram technique was also used [144], which, however, does not look suitable for proteins, when even the order of magnitude of T_2 is unclear and when the representation of a protein in the form of a crystal is doubtful.

Spin relaxation is often studied within the framework of Redfield's theory [145], whence it follows that the relaxation matrix describing relaxation transitions depends on energy level differences, and therefore on the MF magnitude. Under the influence of perturbations, the rates of some transitions, when the external MF decreases to magnitudes much smaller than the HFI field, which is the GMF level, can increase significantly, while those of other transitions can decrease to zero, as shown in [141]. There, calculations were carried out of probabilities of relaxation transitions (a) in some spin states, (b) at a nonzero MF, (c) mainly for T_1, and (d) in the case of radicals in a medium different from the quasisolid state of proteins. It is difficult to use the obtained results to estimate a single decoherence time τ in a zero MF, because it is determined by contributions of all transitions. Furthermore, there is no preferred axis in a zero MF, and the meaning of longitudinal relaxation is unclear. If the relaxation rate $1/T_1$ is defined as the rate at which populations of different-energy levels tend to equilibrium values, then it should decrease approximately proportionally to the population difference, i.e., tend to zero with decreasing MF. But we are interested in phase relaxation, to which this limitation does not apply.

In general, in the absence of an MF, part of the Zeeman levels degenerate, transitions into them become possible, and the decoherence rate can increase. According to [146], relaxation in high MFs is slower than in low ones. Moreover, degeneracy of quantum levels in a zero MF implies enhancement of spin–orbit effects, which also leads to acceleration of decoherence [117]; for many ion-radicals in nonpolar solvents, this time is 5–20 ns [28]. Redfield's theory was used to analyze the spin relaxation time of oxyradicals in liquid in [118], although without numerical estimates. The authors of [147] calculated the dependence of the rate of some singlet–triplet transitions initiated by random perturbations of HFI constants and found that the probability of $T_0 - S$ transitions decreases to zero in a zero MF; we show in what follows that decoherence via the HFI channel in a zero MF occurs due to transitions in T-states.

The decoherence time in the MF via the HFI channel was estimated in [148] by reducing the equations of quantum dynamics with phenomenological dissipation to Bloch-type equations. An estimate of the order of milliseconds was obtained. True, the author introduced a nonstandard definition of decoherence, to be distinguished from dephasing. At the same time, the dephasing rate was assumed proportional to the MF. In a zero MF, it turns to zero, which is counterintuitive in view of the existence of spin decoherence in the case where the MF is absent altogether. In the GMF, the dephasing time was about 40 ps. In [134], the contribution of relaxation to the chemical kinetics via the exchange interaction channel in geminate recombination was estimated analytically, albeit in conditions quite different from those for RPM processes in proteins.

In [149], spin relaxation of radicals in cryptochrome protein under random variations of the distance between radicals was studied; the average distance was 1.9 nm. With the correlation time of random Gaussian variations in the distance equal to 1 ns, the calculated spin relaxation rate in the RPM via the exchange interaction channel was 2.7×10^8 s^{-1}, which is three orders of magnitude faster than via the dipole–dipole interaction channel. This corresponds to a decoherence time of about 4 ns. The authors show that fluctuations of the exchange interaction at a lower relaxation rate, of the order of 10^7 s^{-1} (decoherence time 100 ns), could contribute to expanding the range of model parameters ensuring the sensitivity of the RPM compass. However, arguments confirming the existence of such a decoherence time are not presented.

As we can see, there are no successful direct analytic calculations of τ of presumably magnetosensitive radical pairs in proteins so far. In indirect estimates from a comparison of theory and experiment, in general, it was assumed in all the above-mentioned studies that, if magnetic effects are observed, then unrealistically large times τ, used in RPM simulations of the effect, correspond to real values. The authors do not offer alternative explanations for the observed magnitude of RPM effects in biology.

As stated above, it is usually assumed in the RPM models of magnetoreception that the spin decoherence time is large, larger than the time of the chemical process, which allows removing the value of τ from theory. It is obvious that, in the absence of precise knowledge about the value of τ, the theoretical model should have contained this parameter: in the Liouville–von Neumann equation, besides terms describing spin-selective reactions, a relaxation term should also be present, representing the Neumann–Lindblad equation. However, until now, as far as we know, no analytic solution of such an equation has been proposed that would explicitly show the competitive influence of the rates of a spin-selective reaction and thermal relaxation on the magnitude of the magnetic effect. What is more, information about the decoherence rate of radicals in proteins in a zero MF is contradictory and is the subject of further research.

Below, we obtain functional relations for the RPM effect in the range of weak MFs with an explicit dependence of the effect magnitude on the spin decoherence rate. A comparison with known experimental data suggests that, in cryptochrome-like proteins, decoherence times of spin pairs are plausible in the range of 3–30 ns. Decoherence times via

channels of hyperfine, Zeeman, spin–orbit, and exchange interactions are estimated, and the smallness of the magnitude of the primary magnetic effect is thereby shown.

2. Magnetic RPM effect with spin relaxation taken into account

In this section, we focus on the effect of changing the populations of singlet–triplet states of a radical pair, without specifying the subsequent stage of chemical kinetics and magnetic signal transduction. It is thereby assumed that the integral MF-induced variation in the fractions of singlet–triplet components leads, via some spin-selective reaction, to the observed effects.

We show how spin relaxation caused by decoherence and chemical kinetics influences the magnetic RPM effect when they occur simultaneously. We trace the evolution of the state of the radical pair ensemble from its creation to disappearance due to chemical kinetics. We use a frequent idealization where the spatial motions of the radical pair are accounted for phenomenologically in the spin Hamiltonian [27, p. 114]. The Liouville–von Neumann equation for the density operator of an idealized spin system with magnetic interactions is supplemented by terms associated with the relaxation and chemical kinetics. We assume that the radicals are separated by a distance sufficient to neglect the magnetic dipole and exchange interactions, which usually reduce the possible magnetic effect. Among the magnetic interactions, we take only the Zeeman and the isotropic part of the hyperfine interaction into account in a 'minimal' system of two electrons and one nucleus coupled to one electron.

The Hamiltonian of the idealized Hamiltonian system, expressed in units of $\hbar$, is

$$-\gamma H(S_z^1 + S_z^2) + a\,\mathbf{I}\mathbf{S}^1\,, \tag{2}$$

where S_i^1 and S_i^2 are the operators of the i-projection of the spins of electrons 1 and 2, a constant MF H is directed along the z-axis, $\gamma \approx 1.76 \times 10^7\ \mathrm{G^{-1}\ s^{-1}}$ is the gyromagnetic ratio of the electron, $\mathbf{I}$ is the nuclear spin operator of the first electron, and a is a constant of the contact hyperfine interaction of the nucleus and electron, expressed in frequency units; the Gaussian system of units is used. The analytic solution for the density matrix ρ of a system with a Hamiltonian of type (2) was investigated in [146]. Electrons of intermediate radicals in a protein usually interact with several nuclei, which reduces the magnetic effect. Model (2) with one nucleus allows estimating the most important properties of the RPM effect, in particular, its maximum possible magnitude.

The contribution of the kinetics of spin-selective chemical reactions to the evolution of the density matrix ρ is taken into account using the anticommutator $-(1/2)\{\kappa P + \kappa' P', \rho\}$, where κ and κ' are the rates of the chemical process through singlet and triplet channels, and P and P' are projectors onto singlet and triplet states [150, 151].

Thermal perturbations cause spin relaxation by modulating various interactions, resulting in the density matrix ρ relaxing to a final thermalized state ρ_∞. This process is accounted for below in the form of a phenomenological dissipator $\propto \rho - \rho_\infty$ [145].

2.1 Liouville–von Neumann equation

It is convenient to take the hyperfine interaction constant a as a frequency unit and use the following notation for the dimensionless time t, MF h, kinetics rates k, and thermal relaxation g:

$$t \equiv at'\,,\quad h \equiv \frac{\gamma H}{a}\,,\quad g \equiv \frac{\Gamma}{a} = \frac{1}{a\tau}\,,\quad k \equiv \frac{\kappa}{a}\,,\quad k' \equiv \frac{\kappa'}{a}\,. \tag{3}$$

Here, t' is time and Γ is the damping constant, inversely proportional to the thermal relaxation time. By order of magnitude, the isotropic HFI constant of radicals in proteins, in MF units, is 0.1–1 mT [30, 88, 152, 153], which is approximately an order of magnitude greater than the GMF magnitude $H_{\mathrm{geo}} \sim 0.05$ mT. Let the isotropic HFI constant in frequency units be $a \equiv \gamma\, 10 H_{\mathrm{geo}} \approx 8.8 \times 10^7\ \mathrm{s^{-1}}$. The geomagnetic field then corresponds to $h = 0.1$, which is convenient, and a unit of dimensionless time $t = at'$ corresponds to the time $1/a = 11.4$ ns. The thermal relaxation time τ at $g = 1$ is equal to the same value.

In terms of the notation in (3), in the absence of chemical kinetics, we write the equation for an open quantum system, the Liouville–von Neumann equation with a dissipator, or the Lindblad equation, in the form

$$\begin{aligned} &\partial_t \rho = -\mathrm{i}[\mathcal{H}, \rho] - g(\rho - \rho_\infty)\,,\\ &\mathcal{H} \equiv -h(S_z^1 + S_z^2) + \mathbf{I}\mathbf{S}^1\,, \end{aligned} \tag{4}$$

where ∂_t is the time derivative operator, $\mathcal{H}$ is the Hamiltonian, and $[\,,]$ is the commutator. Spin relaxation is represented by a dissipator proportional to g. Because in a weak MF the Zeeman splitting is much smaller than $k_{\mathrm{B}}T$, ρ_∞ is the density matrix of a fully mixed state. In the matrix representation, in accordance with the dimension of the spin space of the three-spin system, ρ_∞ is an eight-row normalized identity matrix $1/\mathrm{tr}\,(1)$. Equation (4) preserves the unit trace of the density matrix.

In the presence of chemical kinetics, the trace is not conserved; it tends to zero [150]. This should also be taken into account in the dissipator, where, instead of the equilibrium density matrix ρ_∞, we must use the reduced matrix $\mathrm{tr}\,(\rho)\rho_\infty$. This assumes that the relaxation rate is much greater than the characteristic rate of the spin dynamics. The dissipator then has the form $-g[\rho - \mathrm{tr}\,(\rho)\rho_\infty]$. To analyze the joint action of thermal relaxation and the chemical kinetics on the RPM effect, we use the following equation for a quantum system where the chemical kinetics and relaxation are taken into account phenomenologically:

$$\partial_t \rho = -\mathrm{i}[\mathcal{H}, \rho] - \frac{1}{2}\{kP + k'P', \rho\} - g\big[\rho - \mathrm{tr}\,(\rho)\rho_\infty\big]\,. \tag{5}$$

In the particular case $k = k' = 0$, we have $\mathrm{tr}\,(\rho) = 1$, and the above equation reduces to (4).

In numerical simulations of the RPM compass to account for spin relaxation, a Lindblad superoperator with equal dissipation coefficients is sometimes used [149, 154, 155]. As is shown below, the use in (5) of a dissipator in the Lindblad form $(1/2)\sum_i g_i([L_i\rho, L_i^+] + [L_i, \rho L_i^+])$ (see, e.g., [156, p. 447]), with a common coefficient $g_i = g/2$, where the summation ranges all spin operators L_i of the three-spin system, gives results practically indistinguishable from those corresponding to the simple dissipator $-g[\rho - \mathrm{tr}\,(\rho)\rho_\infty]$, which justifies its use in (5).

2.2 Magnitude of RPM effect

Unlike (4), Eqn (5) does not have an analytic solution in general. We first consider the frequently used approximation

$k' = k$ (see, e.g., [30, 97, 136, 139, 140, 154]), which allows an analytic solution. At $k' = k$, because the sum of projectors onto the singlet and triplet subspaces is equal to the identity operator, the chemical term in Eqn (5) is $-k\rho$. It describes the tendency toward an exponential decay of the density matrix.

Analytic solutions of an equation like (5) at $k' = k = 0$ were studied in [101, 145] and elsewhere, and at $g = 0$, in [153] and other papers cited in the Introduction. Numerical solutions of equations similar to (5) with a Lindblad-type dissipator were obtained, e.g., in [149, 154]. An analytic solution of Eqn (5) with chemical kinetics and, conjunctively, with dissipation was obtained in [73, 157],

$$\rho = (U\rho_0 U^+ - \rho_\infty)\exp\left[-(g+k)t\right] + \rho_\infty \exp(-kt)\,, \quad (6)$$

where $U(t) \equiv \exp(-\mathrm{i}\mathcal{H}t)$.

Let a pair of spin-correlated electrons be produced in a singlet state with a density matrix $\rho_0 = P/\mathrm{tr}\,(P)$. Dissipation, the chemical kinetics, and the action of the MF cause transitions between different quantum states of the system: quantum beats, or oscillations. As a consequence, the fraction of the singlet state, from which the process of radical recombination is possible, decreases.

We are interested in the population of the singlet state $\rho_\mathrm{s} \equiv \mathrm{tr}\,(P\rho)$, whose behavior characterizes the magnetic effect. With the notation $F \equiv \mathrm{tr}\,(PU\rho_0 U^+)$ and, because in the considered case of a three-spin system $\mathrm{tr}\,(P\rho_\infty) = 1/4$, it follows from (6) that

$$\rho_\mathrm{s}(t,k,g) = \frac{\exp(-kt)}{4} + \left[\rho_\mathrm{s}(t,k,0) - \frac{\exp(-kt)}{4}\right]\exp(-gt)\,, \quad (7)$$

$$\rho_\mathrm{s}(t,k,0) \equiv \exp(-kt)F(t)\,,$$

where $\rho_\mathrm{s}(t,k,0)$ is ρ_s in the absence of relaxation, and the variable h is omitted for convenience. A reasonable analytic representation of ρ_s, as well as of F, is not always possible and is determined by the choice of basis, the simplicity of the Hamiltonian, and the initial density matrix. Here, the Zeeman basis is used, constructed from tensor products of eigenvectors of the operator S_z in the spin spaces of two electrons and the nucleus.

In the absence of kinetics, $k = 0$, and then Eqn (7) takes the form $\rho_\mathrm{s}(t,0,g) = 1/4 + [\rho_\mathrm{s}(t,0,0) - 1/4]\exp(-gt)$. This relation was proposed in [28] to account for spin relaxation in the RPM model of quantum beats. It is based on the semiempirical assertion that, in the presence of relaxation, ρ_s tends to the equilibrium value $1/4$ starting from $\rho_\mathrm{s}(0,0,0) = 1$. Because the relation $\rho_\mathrm{s}(t,0,g) + \rho_\mathrm{t}(t,0,g) = \mathrm{tr}\,(\rho) = 1$ holds at $k = 0$, where $\rho_\mathrm{t}(t,0,g)$ is the triplet component, it follows from Bagryansky's formula that $\rho_\mathrm{t}(t,0,g) = 3/4 + [\rho_\mathrm{t}(t,0,0) - 3/4]\exp(-gt)$. In [49], this relation was used to account for relaxation, albeit, in a model with kinetics, i.e., it assumed setting (formula (3) in the above paper)

$$\rho_\mathrm{t}(t,k,g) = \frac{3}{4} + \left[\rho_\mathrm{t}(t,k,0) - \frac{3}{4}\right]\exp(-gt)\,.$$

This relation leads to the value $3/4$ at the end of evolution, which is incorrect, because the relation $\rho_\mathrm{t}(t,k,g) + \rho_\mathrm{s}(t,k,g) = \mathrm{tr}\,(\rho) = \exp(-kt)$ holds at $k \neq 0$, and therefore $\rho_\mathrm{t}(t,k,g) \to 0$ as $t \to \infty$.

Next, we must explicitly specify all arguments of the functions F and ρ_s: $F = F(t,h)$ and $\rho_\mathrm{s} = \rho_\mathrm{s}(t,h,g,k)$; we recall that g and k are the rates of the spin-relaxation and kinetic processes. We can calculate the evolution operator $U \equiv \exp(-\mathrm{i}\mathcal{H}t)$ and $F(t,h) \equiv \mathrm{tr}\,(PU\rho_0 U^+)$ by diagonalizing the Hamiltonian $\mathcal{H}$ in (4). Or, even simpler, because $\rho_0 = P/\mathrm{tr}\,(P) = P/2$ and $P = \sum_i |\sigma_i\rangle\langle\sigma_i|$, where σ_i are electrons-singlet states with different nuclear spin projections, we obtain $2F = \sum_{i,k} |\langle\sigma_i|U|\sigma_k\rangle|^2$. Omitting intermediate calculations, we write the result:

$$F(t,h) = \frac{1}{2} - \frac{1}{8\eta^2} + \frac{\cos(t\eta)}{8\eta^2} + \frac{\cos(t\eta/2)\cos(t/2)\cos(ht/2)}{2} + \frac{h\sin(t\eta/2)\cos(t/2)\sin(ht/2)}{2\eta}\,, \quad \eta \equiv \sqrt{h^2+1}\,. \quad (8)$$

The singlet component $\rho_\mathrm{s}(t,h,g,k)$ is derived by substituting F in (7).

The time dependences of the singlet state population ρ_s, calculated using formulas (7) and (8), are presented in Fig. 2a. Similar oscillations (quantum beats due to interference effects, analogous to Torrey oscillations in pulsed EPR [158]) are well known (see, e.g., [151, 159]) and are observed experimentally, constituting the subject of a powerful research method (see, e.g., [28, 160]). At the beginning of spin evolution, Eqn (7) yields $U = 1$, $F = \mathrm{tr}\,(P\rho_0) = 1$, and $\rho_\mathrm{s} = 1$, and hence the system is in a singlet state, as was

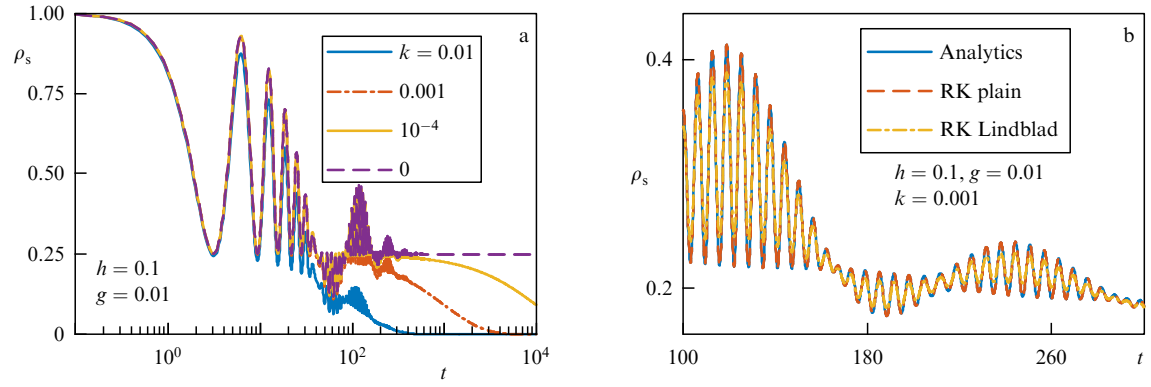

Figure 2. Quantum oscillations of singlet state population $\rho_\mathrm{s}(t,h,g,k)$: (a) calculation by formula (7) at different values of chemical kinetic rate k; (b) calculation by formula (7) and by RK method for simple and Lindblad dissipators. Values of step and integration time interval, 0.003 and 10^4, respectively, ensured convergence and accuracy of RK procedure.

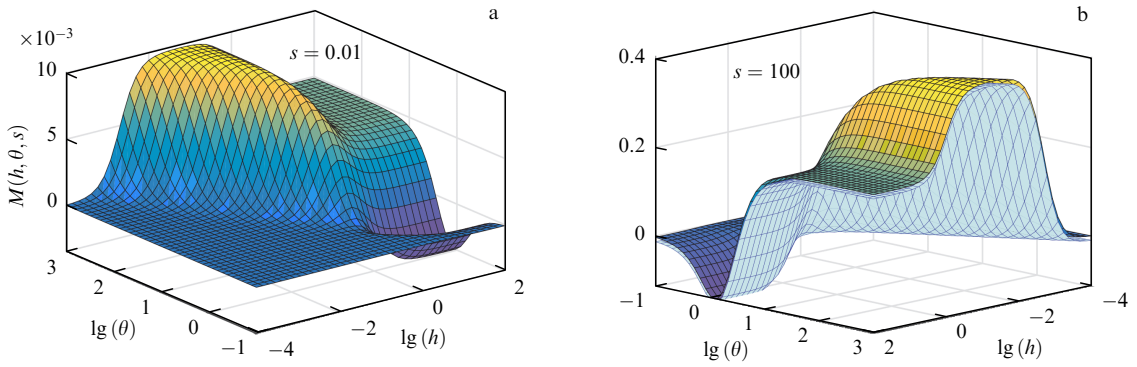

Figure 3. Dependence of RPM effect on MF h and parameter $\theta = 1/(g+k)$ for values of s differing by four orders of magnitude, in different projections; (a) calculation by formula (11), (b) calculation by formula (11) (upper layer) and using solution of Eqn (5) by RK method (lower layer). For better distinction, layers are slightly shifted along vertical axis.

determined by the choice of the initial density matrix ρ_0. At the end of evolution, $\rho_s = 0$, except in the case of the absence of chemical kinetics $k = 0$.

Figure 2b shows the time evolutions of ρ_s calculated using formula (7) and by numerical integration of Eqn (5) using the Runge–Kutta (RK) method for a simple dissipator and the Lindblad dissipator. It can be seen that the curves obtained by the analytic and numerical calculations coincide. This confirms the validity of the analytic solution and the accuracy of the numerical procedure, which is used further in the case $k' \neq k$ as well. In addition, the dissipators (the simple and Lindblad ones) give a practically identical result, which justifies the use of the simple dissipator in Eqn (5).

The integral magnetic effect considered below depends on the fine structure of oscillations $\rho_s(t)$ (see Fig. 2). The coherence of spin states, determined by the relaxation rate g, is reflected in the structure of oscillations and therefore has a strong influence on the magnitude of the magnetic effect.

How is the magnetic effect defined? Usually, such that it can be related to a quantity measured in experiment, i.e., by somehow averaging the dependence $\rho_s(t)$ over a time interval significantly exceeding the period of fast oscillations visible in Fig. 2. In RPM models, a definition of the magnetic effect in the form of an averaged fraction of singlet radical pairs is often used (see, e.g., [82, 153]):

$$k\int_0^\infty \exp(-kt)\,\rho_s(t,h,k)\,\mathrm{d}t\,. \tag{9}$$

This definition, where the averaging 'window' is determined by the rate of the chemical kinetics, would make sense for a phenomenological account for the decay of the density matrix due to the kinetic process if the equation of spin dynamics did not contain Haberkorn terms. In our case, the common exponential $\exp(-kt)$ is already included in solution (6) of Eqn (5), and its repeated use for averaging makes no sense. In this paper, we study RPM effects in a weak MF of the order of the GMF. It is therefore convenient to define the magnetic effect such that it be positive in small MFs and relative to the situation where the MF h is absent. Setting $k > 0$, we write the magnetic effect in the form

$$M(h) \equiv 1 - \frac{\int_0^\infty \rho_s(t,h,g,k)\,\mathrm{d}t}{\int_0^\infty \rho_s(t,0,g,k)\,\mathrm{d}t}\,. \tag{10}$$

With this definition, $M(0) = 0$, and the MF h changes this value such that, for example, $M = 0.1$ implies a 10% effect. It is essential in this definition that $k \neq 0$; otherwise, the fraction of the singlet component at $t \to \infty$ would tend to 1/4 (Fig. 2a) and the integrals would diverge. However, the situation where the kinetics in the RPM can be neglected and one can set $k = 0$ makes no sense for magnetobiology, because the product vanishes, and hence so does the channel of MF influence on biological measured quantities. A possible definition of M in terms of the triplet component $\rho_t \equiv \mathrm{tr}(\rho) - \rho_s$ leaves the results practically unchanged.

A fortunate choice of variables simplifies the problem and often makes its analytic solution possible. Here, such variables are $\theta \equiv (g+k)^{-1}$ and $s \equiv k/g$; they respectively determine the total characteristic time of the density matrix reduction and the asymmetry of the rates of chemical kinetics and thermal relaxation. It turns out that θ and s are the respective parameters of shape and the scale of magnetic dependences.

Calculating the integrals in (10) gives a result that in compact explicit form can be written as

$$M(h,\theta,s) = \frac{A_1(h,\theta)}{A_2(h,\theta)}\,B(\theta,s)\,, \tag{11}$$

where $B(\theta,s) \equiv s\theta^4/(8s + 5s\theta^2 + 2\theta^2 + 2)$ and

$$\begin{aligned} A_1(h,\theta) &\equiv h^2(h^4\theta^8 - 4h^4\theta^6 - 32h^4\theta^4 + 2h^2\theta^8 + 6h^2\theta^6 \\ &\quad - 12h^2\theta^4 - 64h^2\theta^2 + 8\theta^6 + 16\theta^4 - 24\theta^2 - 32)\,, \\ A_2(h,\theta) &\equiv (h^2\theta^2 + \theta^2 + 1)(h^2\theta^4 + 4h^2\theta^2 - 4h\theta^2 + 4\theta^2 + 4) \\ &\quad \times (h^2\theta^4 + 4h^2\theta^2 + 4h\theta^2 + 4\theta^2 + 4)\,. \end{aligned}$$

The dependence $M(h,\theta,s)$ is shown in Fig. 3 on a logarithmic scale along the axes h and θ for two values of s. The magnetic effect can be positive (this is a decrease in the time-averaged singlet component ρ_s when the MF is switched on) and negative. We can see that the shape of the surface depends little on the ratio of rates $s = k/g$. The parameter s mainly controls the overall magnitude of the effects, which follows from a comparison of the vertical scales of the dependences in Fig. 3a and 3b and from the form of the function $B(\theta,s)$ in (11).

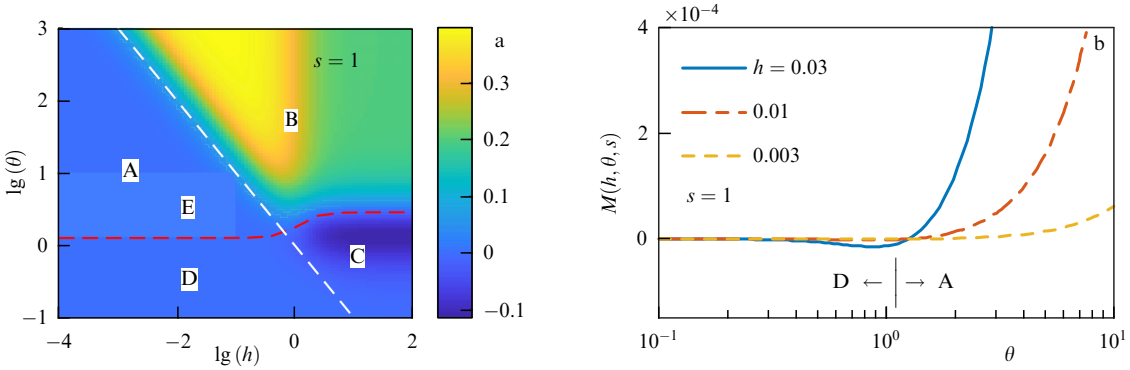

Figure 4. (a) Distribution of magnetic effects by magnitude depending on values of parameters h and θ. A, B, C, D: regions of qualitatively different effects. White dashed line: $\theta = 1/h$, red dashed line: zero effect line $M(h, \theta, s) = 0$. (b) θ-dependence of magnetic effect at different values of weak MF. In weak MF, boundary between A and D is determined by equality $\lg(\theta) \approx 0.097 (\theta = 1.25)$.

2.3 Regions of RPM effects

Let us consider solution (11) in more detail. There are different regions of variation of the parameters h and $\theta \equiv (g + k)^{-1}$ (Fig. 4a): those where magnetic effects differ either in sign or significantly in magnitude. The tilted dashed line $h\theta = 1$, or $h \sim g + k$, separates regions B and C of relatively large effects from regions A and D of orders-of-magnitude lower effects. This relation means that the sum of thermal and kinetic rates corresponds to the electron spin precession frequency γH.

By definitions (3), the equation $h \sim g + k$ for quantities with physical dimensions is $\gamma H\tau \sim 1 + \kappa\tau$, where τ is the spin decoherence time. This is a fundamental relation of a more general kind. At a low rate of chemical kinetics $\kappa\tau < 1$, we have $\gamma H\tau \sim 1$. This equality (1), as shown in the Introduction, follows from the most general quantum principles, and the RPM, of course, obeys it. But if the rate of the chemical kinetics is greater than the spin decoherence rate, i.e., $\kappa\tau > 1$, then it is exactly what determines the critical MF, $\gamma H \sim \kappa$, when magnetic effects become large.

The almost horizontal dashed line in Fig. 4a, the line of zero effects, is the solution of the equation $M(h, \theta, s) = 0$, which determines the equation for the dashed line $\theta(h, s)$; it separates the regions A and B of positive and the regions C and D of negative effects.

Large magnetic chemical effects of regions B and C, of the order of 10–30%, are observed in spin-chemical experiments in MFs in the range of tens of mT or more. It would seem that large effects of region B could also be observed at small MFs $h \sim 0.1$ (upper yellow zone of this region). However, the values of $\lg(\theta)$ would have to exceed unity in that case, or $g + k \lesssim 0.1$, which is hardly realistic. For this, it is necessary, at least, that $g < 0.1$, i.e., $\tau = 1/(ag) \gtrsim 100$ ns, which is improbable. As stated above, thermal spin relaxation times of unpaired electrons in proteins exceeding 100 ns at physiological temperatures are often assumed by default when explaining magnetic effects within the framework of the RPM. However, experimental evidence of such slow relaxation of the spins of the considered radicals has not yet been obtained.

Negative effects in region D (Fig. 4b) are orders of magnitude smaller than effects in A. Consequently, to explain biological effects of the MF at the GMF level or lower, only a narrow lower subregion of region A is relevant; this is a strip bounded by the inequalities $0.1 \lesssim \lg(\theta) \lesssim 1$ and $\lg(h) \lesssim -1$. In Fig. 4a, it is highlighted with a slightly less dense color in region A and denoted by E.

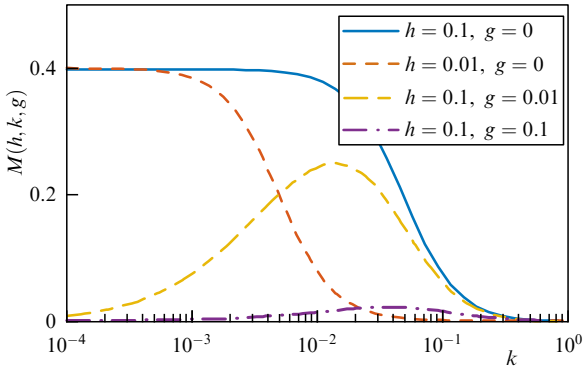

Figure 5. Dependence of magnetic effect on rate of chemical kinetics k at different MFs and spin relaxation rates. Value $g = 0.01$ corresponds to relaxation time $\tau \approx 1$ μs, and $g = 0.1$, to time $\tau \approx 100$ ns.

In Fig. 4a, there is a surprising section in region C, between the red dashed line of the zero RPM effect and the middle of the dark blue region. There, an increase in the spin relaxation rate g accompanied by a decrease in $\lg(\theta)$ leads to a 'paradoxical' growth of the absolute value of the magnetic effect. This means that spin relaxation, generally speaking, can facilitate the magnetic effect rather than inhibit it. We note, however, that the entire region C is one of large effects in the MF exceeding 0.5 mT. It is located far from region E of effects that are actually observed in weak MFs, and therefore hardly relates to magnetobiology.

The magnetic effect in terms of the original variables k and g is obtained from (11) by substitutions $\theta = 1/(k + g)$ and $s = k/g$. The dependences $M(k)$ at different values of h and g are shown in Fig. 5. In the absence of spin relaxation ($g = 0$), the effect appears at a rate of chemical kinetics of the order of the spin precession rate $k \sim h/2\pi$ (or $\kappa \sim \gamma H_{\text{geo}}/2\pi \approx$ 1.4 MHz). If relaxation takes place, then the rate k of the kinetics delivering the maximum effect depends on g such that, at low rates $k \ll g$, the magnetic effect practically disappears.

2.4 Spin relaxation dampening 'low-field effect'

There are many studies where large effects in region B are investigated theoretically in the hope of explaining the magnetic orientation of animals [159] and nonspecific

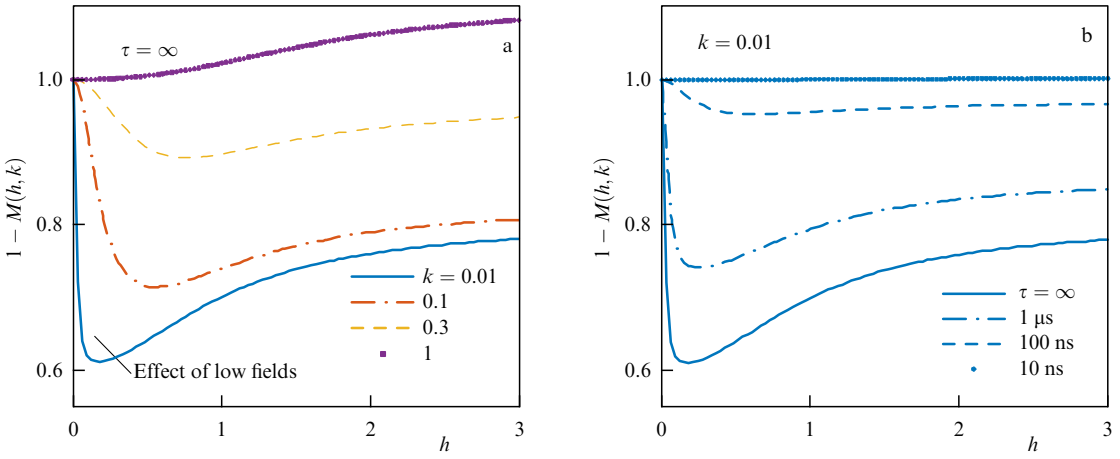

Figure 6. Dependence of singlet yield of reaction via RPM mechanism on MF magnitude (a) in absence of and (b) in presence of spin relaxation at different values of chemical reaction rate k and relaxation time τ; calculation is based on formula (11).

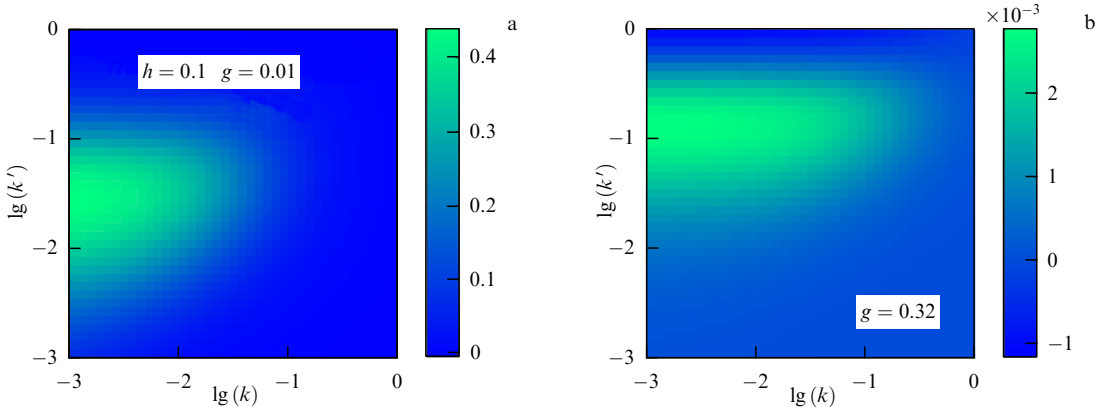

Figure 7. Dependence of magnetic effect on chemical kinetic rates in singlet k and triplet k' channels at GMF $h = 0.1$ and spin relaxation time of about (a) 1 μs and (b) 36 ns.

magnetic effects observed in biological experiments [13]. The magnetic effect is typically defined by the singlet yield, which in our case is equal to $1 - M(h)$, and spin relaxation is disregarded. The dependence on the MF magnitude obtained in this way is well known (see, e.g., [45, 119, 153]). It follows from (11) at $g = 0$, or $s \to \infty$, i.e., assuming the absence of thermal relaxation (Fig. 6a). The initial drop in the singlet yield is called the low-field effect [146]. It can be seen that, at a low kinetic rate k, noticeable RPM effects could already be achieved in very small fields $h \ll 1$, as, for example, in [97]: a 30% calculated effect when varying the MF in the hypomagnetic range from 0 to 5 μT. However, such an assertion is incorrect and is a consequence of ignoring spin relaxation. As can be seen from Fig. 6b, the low-field effect quickly disappears with a decrease in the relaxation time τ. At reasonable relaxation time values $\tau <$ 10–100 ns, the effect when varying the MF by the GMF magnitude does not exceed tenths of a percent.

Magnetic effect at $k \neq k'$. Formula (11), obtained analytically, is valid when the rates of the kinetics through singlet and triplet channels are equal, $k' \sim k$. This case is illustrative in the analysis of the contribution of thermal relaxation to the RPM effect. It is also interesting to understand magnetic effects in the practically important case $k' \neq k$, when an analytic solution of Eqn (5) is impossible. Below, we give the results of calculating M based on a numerical RK integration of this equation at $k \in [10^{-3}, 1]$ and $k' \in [10^{-3}, 1]$ and different spin relaxation rates (Fig. 7).

We can see that both low and high kinetic rates through the triplet channel suppress the magnetic effect. The value $k' \approx 0.05$, which gives the maximum effect, depends little on k. The calculation of M in region E in Fig. 4a shows that, also in the case of different rates k and k', the quadratic dependence of the effect on the MF is preserved in the region of low fields $h < k + g$. It is also seen that shifting the relaxation time from values of the order of 1 μs to a value 30 times smaller, which is more probable in a protein medium, leads to a sharp decrease in M by more than two orders of magnitude and to a slight increase in the maximizing value of k' from 0.05 to 0.2. The values of $k' \sim 0.1$ in frequency units are $k'a \sim 10^7$ s^{-1}.

Initial state of radical pair. The magnitude of the RPM effect depends on the initial state of the pair. In particular, with an equilibrium initial state, the magnetic effect should be absent. Everywhere in the foregoing, as in all studies on the RPM effect in magnetic biology, it was assumed that the initial state of the pair is singlet or triplet. But how good is such an idealization? If the pair is produced, for example, by the breaking of a covalent bond, then the angular momentum conservation law dictates an initial singlet state. But the emergence of radical pairs upon photoexcitation of flavin is

different (see Fig. 1). The radicals of the first pairs are separated by relatively small distances, which means a large exchange interaction and therefore fast decoherence of the FAD radical. In [59], the decoherence time in the radical pair FAD–Trp, separated by a distance of 1.32 nm, was estimated to bet 10 ps. Consequently, the initial state of the next (magnetically sensitive) pair could be equilibrium. However, the high decoherence rate is compensated by the small picosecond lifetimes of these pairs [161], and significant decoherence, apparently, does not have time to build up. Therefore, the idealization of the singlet initial state is acceptable, although the absence of an observed effect could be explained not only by the fast decoherence of the magnetically sensitive pair described by Eqn (5) but also by significant decoherence of the preceding pairs.

3. Spin decoherence

Because the spin decoherence time is a decisive factor for the emergence of observable (i.e., of a sufficiently large magnitude) magnetic effects, it is interesting to obtain estimates of this time analytically from general considerations. The decoherence time of radicals depends on the MF magnitude. However, we limit ourselves to considering the RPM effects in weak MFs at the geomagnetic level, 1 to 2 orders of magnitude smaller than typical HFI fields. In such small MFs, the Zeeman multiplet is partly degenerate, and the phase relaxation time becomes the spin decoherence time. It then makes sense to estimate the decoherence in a 'zero' MF, which simplifies calculations. We note that the Redfield theory for the spin relaxation matrix is redundant when applied to simple systems, due to cumbersome mathematics. We are interested in orders of magnitude, which justifies the use of simplified models of spin dynamics. At the same time, the obtained solutions are exact.

Calculated below are the decoherence times arising from hyperfine, Zeeman, spin–orbit, and exchange interactions modulated by thermal fluctuations of the medium. The most probable channel of fast relaxation is determined. The results are of a general character and can be extended to a system of chemically reacting spin-correlated electrons within the RPM theory framework. In this section, it is more convenient to perform calculations while keeping the physical dimensions of quantities.

3.1 Hyperfine interaction channel

Here, we consider the simple case of a radical with one nucleus and an isotropic HFI, with a constant a, modulated by random perturbations. In a weak MF, $\gamma H \ll a$ (see (3)), and we therefore assume it vanishes and neglect the Zeeman interaction in (2). Let the spin Hamiltonian of a contact HFI, due to nonzero electron density at the magnetic nucleus,

$$\mathcal{H}_{\rm hf}(t) = \mathcal{H}_0 + V(t) \equiv \hbar a \sum_i S_i I_i + \sum_i v_i(t) S_i I_i\,, \quad i = x, y, z\,, \tag{12}$$

contain a constant part $\mathcal{H}_0$ and a random part $V(t)$. In this form, the perturbation V is partly anisotropic; otherwise, all v_i would be identical and would not induce transitions. The perturbation operator $V(t)$ includes random processes $v_i(t)$, which are assumed to be stationary and are understood in the sense of generalized functions.

If the stationary random process $v(t)$ is represented as a Fourier transform $v_t = \int v_f \exp(\mathrm{i}2\pi f t)\,\mathrm{d}f$, where v_f are spectral amplitudes, then, according to the Wiener–Khinchin theorem, the autocorrelation function $\langle v_t^* v_{t+\tau}\rangle$ is $\int Q(f)\exp(\mathrm{i}2\pi f\tau)\,\mathrm{d}f$, where $Q(f)$ is the power spectral density, such that $\int Q(f)\,\mathrm{d}f \equiv \sigma_v^2$, and σ_v^2 is the variance of the process v_t. Below, the idealization of a uniform spectrum of thermal perturbations relevant to the problem is adopted, i.e., $Q(f) = q = \text{const}$. Then, $\langle v_t^* v_{t+\tau}\rangle = q\int \exp(\mathrm{i}2\pi f\tau)\,\mathrm{d}f = q\delta(\tau)$, where $\delta(...)$ is the Dirac delta function. In contrast to white noise with infinite variance, we assume that the spectrum width is bounded, $f \in (-f_0, f_0)$, i.e., $q = \sigma_v^2/2f_0 = \sigma_v^2\tau_{\rm c}$, where $\tau_{\rm c}$ is the autocorrelation time of perturbations. We also assume that the spectral density of perturbations q is the same for all components v_i, which are considered independent,

$$\langle v_i(t)\rangle = 0\,, \quad \left\langle v_i^*(t) v_k(t')\right\rangle = q\,\delta_{ik}\delta(t-t')\,, \tag{13}$$

where δ_{ik} is the Kronecker symbol. This is a very good idealization, given that the correlation time of thermal perturbations is orders of magnitude smaller than the characteristic time scale of spin dynamics [145]. Angle brackets here and hereafter denote both ensemble averaging and quantum mechanical averaging; the type of averaging is clear from the context.

It seems that, to describe coupled processes of spin decoherence and relaxation without accounting for explicit interaction with a thermostat, the Hamiltonian $\mathcal{H}_{\rm hf}$ must include a phenomenological interaction of the spin with the thermostat. However, in our case, the perturbation operator V does not cause transitions with energy change. In this case, accounting for energy exchange with the thermostat phenomenologically is redundant. Consequently, the presence of damping in the Schrödinger equation $\partial_t\Psi = -(\mathrm{i}/\hbar)\mathcal{H}_{\rm hf}\Psi$ is not necessary. At the same time, as we see in what follows, transitions in degenerate levels under the action of a fluctuating perturbation take place and cause decoherence of the spin dynamics.

It is convenient to move to the basis of eigenfunctions of the operator $\mathcal{H}_0 = \hbar a\sum_i S_i I_i$ in (12). These are the triplet $\phi_0 \equiv |\uparrow\uparrow\rangle$, $\phi_1 \equiv (|\uparrow\downarrow\rangle + |\downarrow\uparrow\rangle)/\sqrt{2}$, $\phi_2 \equiv |\downarrow\downarrow\rangle$ and the singlet $\phi_3 \equiv (|\uparrow\downarrow\rangle - |\downarrow\uparrow\rangle)/\sqrt{2}$ with the respective eigenvalues $\varepsilon_0 = \varepsilon_1 = \varepsilon_2 = \hbar a/4$ and $\varepsilon_3 = -3\hbar a/4$; the arrows indicate the values of the z-projections of electron and nucleus spin in the Zeeman basis. The perturbation operator and its matrix elements in the ϕ basis are

$$V = \frac{1}{4}\begin{bmatrix} v_z & 0 & v_{xy} & 0 \\ 0 & v'_{xy} - v_z & 0 & 0 \\ v_{xy} & 0 & v_z & 0 \\ 0 & 0 & 0 & -v'_{xy} - v_z \end{bmatrix}, \quad V_{kn} \equiv \langle\phi_k|V|\phi_n\rangle,$$

where we set $v_{xy} \equiv v_x - v_y$ and $v'_{xy} \equiv v_x + v_y$. The equation for the coefficients c_k of the expansion of Ψ in stationary states, $\Psi = \sum_k c_k(t)\exp(-\mathrm{i}\varepsilon_k t/\hbar)|\phi_k\rangle$, obtained from the Schrödinger equation, has the standard form [71, p 183; 162] $\partial_t c_k = -(\mathrm{i}/\hbar)\sum_n c_n \exp(\mathrm{i}\omega_{kn}t/\hbar)V_{kn}$, where, due to the degeneracy of triplet levels, all frequencies $\omega_{kn} \equiv \varepsilon_k - \varepsilon_n$ corresponding to nonzero elements V_{kn} are equal to zero, and hence

$$\partial_t c_k = -\frac{\mathrm{i}}{\hbar}\sum_n V_{kn}c_n\,, \quad \text{or} \quad \partial_t \mathbf{c} = -\frac{\mathrm{i}}{\hbar}\,V\mathbf{c}\,, \tag{14}$$

where $\mathbf{c}$ is a four-row column of coefficients. It follows from the form of $V\mathbf{c}$ and from the form of the matrix V that

transitions occur only between states 0 and 2 ($T_+ \leftrightarrow T_-$), and populations of states 1 and 3 do not change. Thus, the dimension of the problem can be reduced to two.

We introduce elements of the reduced density matrix $\rho_{00} \equiv c_0^* c_0$, ρ_{02}, ρ_{20}, ρ_{22}. Setting $\rho_{00} - \rho_{22} \equiv X$, $\rho_{02} - \rho_{20} \equiv Y$, we write the equations implied by (14), $\partial_t X = -\mathrm{i} w Y$, $\partial_t Y = -\mathrm{i} w X$, where $w(t) = v_{xy}(t)/2\hbar$. These equations do not contain v_z and v'_{xy}. Their solution with the initial condition $X(0) = 1$, $Y(0) = 0$, or, equivalently, $c_0(0) = 1$ and $c_2(0) = 0$, is $X(t) = \cos[W(t)]$, $Y(t) = -\mathrm{i}\sin[W(t)]$, where

$$W(t) \equiv \int_0^t w(t')\,\mathrm{d}t' . \tag{15}$$

Because we assumed that $w \propto v_{xy} \equiv v_x(t) - v_y(t)$ corresponds to white noise (see (13)), the function $W(t)$ is a Wiener, or Brownian, process with the variance growing proportionally to t. This does not prevent the calculation of the statistical characteristics of processes X and Y, which are periodic functions of a random argument and, unlike $W(t)$, are stationary at sufficiently large time intervals.

We are interested in the process of loss of electron spin coherence, i.e., the autocorrelation function of the quantum mechanical average of some spin projection. Let this average be $s(t) \equiv \langle S_z \rangle = \mathrm{tr}\,(S_z \rho)$; it is independent of the choice of basis. Having determined the elements of the reduced density matrix from solutions $X(t)$ and $Y(t)$ and reconstructed the four-row density matrix ρ from the reduced one, we obtain, given the above initial conditions,

$$\rho = \frac{1}{2}\begin{bmatrix} 1+\cos W & 0 & -\mathrm{i}\sin W & 0 \\ 0 & 0 & 0 & 0 \\ \mathrm{i}\sin W & 0 & 1-\cos W & 0 \\ 0 & 0 & 0 & 0 \end{bmatrix} . \tag{16}$$

Because $\mathrm{tr}\,(\rho) = \mathrm{tr}\,(\rho^2) = 1$ here, the state of the system remains pure, which is natural, because transitions occur in degenerate states. Using (16) to calculate the trace $\mathrm{tr}\,(S_z\rho)$, where the operator S_z is taken in the basis ϕ, we have

$$s(t) = \mathrm{tr}\,(S_z\rho) = \frac{1}{2}\cos[W(t)] = \frac{1}{2}\cos\left(\int_0^t w(t')\,\mathrm{d}t'\right). \tag{17}$$

The autocorrelator $K \equiv \langle s(t)s(t')\rangle/(\sigma_{s(t)}\sigma_{s(t')})$, considering that the variance σ^2 of sinusoidal random process (17) is equal to $1/8$ due to the statistical properties of w, has the form

$$\begin{aligned} K &= \big\langle \cos\big[W(t) - W(t+\Delta t)\big]\big\rangle + \big\langle \cos\big[W(t) + W(t+\Delta t)\big]\big\rangle \\ &\equiv k_1 + k_2 , \end{aligned} \tag{18}$$

where we set $t' \equiv t + \Delta t$, and the product of cosines is transformed into a sum.

Let us consider the first term. Representing the cosine as a Taylor series and taking (15) into account, we obtain

$$\begin{aligned} k_1 &\equiv \big\langle \cos\big[W(t) - W(t+\Delta t)\big]\big\rangle = \left\langle \cos\left[\int_t^{t+\Delta t} w(t')\,\mathrm{d}t'\right]\right\rangle \\ &= \sum_{k=0}^{\infty} \frac{(-1)^k}{(2k)!}\langle u^{2k}\rangle , \end{aligned} \tag{19}$$

where we use Fubini's theorem to write $\langle u^{2k}\rangle$ as

$$\langle u^{2k}\rangle = \int \ldots \int \big\langle w(t_1)\ldots w(t_{2k})\big\rangle\,\mathrm{d}t_1 \ldots \mathrm{d}t_{2k} . \tag{20}$$

All integrals are taken from t to $t + \Delta t$. For a Gaussian process $w(t)$, according to [163, Eqn (6); 164, pp. 332, 341], the correlator in the integrand can be represented as a sum of products of pairwise correlators

$$\big\langle w(t_1)\ldots w(t_{2k})\big\rangle = \sum \prod \big\langle w(t_1)w(t_2)\big\rangle \ldots \big\langle w(t_{2k-1})w(t_{2k})\big\rangle \tag{21}$$

with summation ranging all possible partitions of the array $w(t_i)$, $i = 1, \ldots, 2k$, into pairs. The number of such partitions is $\prod_{i=1}^{k}(2i-1) = (2k)!/(2^k k!)$ [165; 166, p. 13; 167, p. 41]. Let n denote the partition number. Taking relation (13) into account, i.e., $\langle v_i^*(t) v_k(t')\rangle = q\delta_{ik}\delta(t-t')$, and recalling the realness of the functions $v_i(t)$ and $w(t) = [v_x(t) - v_y(t)]/2\hbar$, we see that the pairwise correlators in (21), denoted as w_{ij}, are equal to

$$\begin{aligned} w_{ij} &\equiv \big\langle w(t_i)w(t_j)\big\rangle = \frac{1}{4\hbar^2}\big\langle [v_x(t_i) - v_y(t_i)]\,[v_x(t_j) - v_y(t_j)]\big\rangle \\ &= \frac{q}{2\hbar^2}\,\delta(t_i - t_j) , \end{aligned} \tag{22}$$

where the definition of q is given in (13). Substituting (21) into (20), using (22), and again applying Fubini's theorem, we obtain the expression

$$\langle u^{2k}\rangle = \sum_n \iint w_{12}\,\mathrm{d}t_1\,\mathrm{d}t_2 \ldots \iint w_{2k-1,\,2k}\,\mathrm{d}t_{2k-1}\,\mathrm{d}t_{2k} , \tag{23}$$

where the summand is the product of k double integrals. Each of them is

$$\frac{q}{2\hbar^2}\iint_t^{t+\Delta t} \delta(t_i - t_j)\,\mathrm{d}t_i\,\mathrm{d}t_j = \frac{q}{2\hbar^2}\,\Delta t \tag{24}$$

and is independent of n. Therefore, the summation over possible partitions in (23) reduces to multiplication by the number of such partitions:

$$\langle u^{2k}\rangle = \frac{(2k)!}{2^k k!}\left(\frac{q}{2\hbar^2}\,\Delta t\right)^k .$$

Substituting this into (19), collecting the resulting series into an exponential, and noting that the second term, k_2, in (18), as an average of the cosine of a random function with zero first moment, vanishes, we conclude that the autocorrelation of the electron spin z-projection has the form

$$K = k_1 = \exp\left(-\frac{\Delta t}{\tau_{\mathrm{hf}}}\right), \quad \tau_{\mathrm{hf}} = \frac{4\hbar^2}{q} = \frac{4\hbar^2}{\tau_{\mathrm{c}}\sigma_v^2} , \tag{25}$$

where τ_{hf} is the spin decoherence time via the HFI channel.

It is also useful to find the time dependence of the average z-projection of spin, $\langle s(t)\rangle = (1/2)\langle\cos(\int_0^t w(t')\,\mathrm{d}t')\rangle$ (see (17)), which determines the spin *relaxation*, not decoherence, time. It follows from (19) that k_1 in this case differs by division by two and the replacement of lower and upper integration limits in (19) with 0 and t. From (24) and (25), we can then immediately write $\langle s(t)\rangle = (1/2)\exp(-t/\tau_{\mathrm{hf}})$. Thus, the rate of spin dynamics decoherence and the rate of spin relaxation (relaxation of the quantity $\langle S_z\rangle \equiv \mathrm{tr}\,(S_z\rho)$ to the equilibrium value 0) are identical in a zero MF. This is exactly what allows accounting for spin decoherence in the Liouville–von Neumann Eqns (4) and (5) phenomenologically in the form of density matrix relaxation.

The decoherence rate in this problem, as seen from (25), is fully determined by the spectral density q of thermal perturbations of contact HFI. Numerical estimates are given in Section 3.3 below.

A similar calculation can be performed for the anisotropic HFI Hamiltonian with axial constants a and b,

$$\mathcal{H}_{\rm hfa} = \hbar a\left[(b+\beta_x)S_xI_x + (b+\beta_y)S_yI_y + S_zI_z\right],$$

where β are random functions of time, $\langle\beta_i\rangle = 0$, $\langle\beta_i(t)\beta_j(t')\rangle = \sigma_\beta^2\tau_{\rm c}\delta_{ij}\delta(t-t')$. The time-dependent perturbation operator in the ST basis has a block form and again allows transitions only between states 0 and 2. The average value of the electron spin z-projection still has the form (17) where, instead of w, we must use $a(\beta_x-\beta_y)/2$. It can be shown that the decoherence time can then be written as

$$\tau_{\rm hfa} = \frac{4}{\tau_{\rm c}(a\,\sigma_\beta)^2},$$

and, with the value of standard deviation of HFI anisotropy fluctuations of the order of $a\sigma_\beta \sim 10$ MHz [168], it differs little from the decoherence time via the isotropic HFI channel.

It is of interest to compare the result in (25) with the decoherence time estimate by Redfield's theory [145]. In it, to describe relaxation processes, a so-called relaxation matrix R is introduced, such that the equation for the density matrix has the form

$$\partial_t\,\sigma_{\alpha\alpha'} = {\rm i}(\alpha'-\alpha)\sigma_{\alpha\alpha'} + \sum_{\beta\beta'} R_{\alpha\alpha'\beta\beta'}\sigma_{\beta\beta'}, \qquad (26)$$

where α are eigenvalues of the Hamiltonian and simultaneously indices of these values. The Hamiltonian is written as $\mathcal{H} = \hbar\mathcal{H}_0 + \hbar G(t)$, where $G(t)$ is the perturbation operator responsible for relaxation due to interaction with the thermostat. Redfield showed that the Schrödinger equation with this Hamiltonian leads to Eqn (26) if we set

$$R_{\alpha\alpha'\beta\beta'} = J_{\alpha\beta\alpha'\beta'}(\beta'-\alpha') + J_{\alpha\beta\alpha'\beta'}(\alpha-\beta) - \delta_{\alpha'\beta'}\sum_\gamma J_{\gamma\beta\gamma\alpha}(\gamma-\alpha) - \delta_{\alpha\beta}\sum_\gamma J_{\gamma\alpha'\gamma\beta'}(\alpha'-\gamma), \qquad (27)$$

where $J_{\alpha\alpha'\beta\beta'}(\omega) = \int_0^\infty \langle G_{\alpha\beta}(t)G^+_{\alpha'\beta'}(t-\tau)\rangle\exp({\rm i}\omega\tau)\,{\rm d}\tau$, the quantities $R_{\alpha\alpha'\beta\beta'}$ are sufficiently small, such that the scale of relaxation times $R^{-1}_{\alpha\alpha'\beta\beta'}$ is much larger than the correlation time of thermal perturbations, and the inverse of $R_{\alpha\alpha'\alpha\alpha'}$ is analogous to the time T_2 in the Bloch equations, i.e., characterizes the spin decoherence time.

Comparing the Hamiltonians $\mathcal{H}$ and $\mathcal{H}_{\rm hf}$ in (12), we see that $G = V/\hbar$, and the eigenfunctions are singlet–triplet states ϕ with the spectrum of eigenvalues of the triplet $\hbar a/4$ and singlet $-3\hbar a/4$. From the form of V in such a basis, it follows that transitions $\pm w$ relate degenerate states 0 and 2, and hence the indices in (27) run through just a couple of values, and all arguments of the J matrices are zero, because they are differences of equal eigenvalues. Then, $J_{0000} = J_{2222} = -J_{0022} = -q/32\hbar^2$, $J_{2020} = J_{0202} = -q/16\hbar^2$, and substitution in (27) shows that $\tau = -R^{-1}_{\alpha\alpha'\alpha\alpha'} = 8\hbar^2/\tau_{\rm c}\sigma_v^2$. This time is twice as large as $\tau_{\rm hf}$ from (25). The discrepancy is explained by the fact that $-R^{-1}_{\alpha\alpha'\alpha\alpha'}$ is not the decoherence time in the exact sense, but the scale of the decoherence time. To calculate τ, we must compute all (in this case, 16) elements of R, solve Eqn (26), and only then find the autocorrelator of the dependence ${\rm tr}\,(S_z\sigma)$ on time. Such a cumbersome procedure is unjustified in the simple illustrative cases we consider, and estimates of decoherence here and below rely on direct solutions of the Schrödinger equations.

3.2 Zeeman, spin–orbit, and exchange channels

Spin decoherence also occurs due to other electron interactions: Zeeman, spin–orbit, and exchange.

Zeeman channel. In a zero external MF, the Zeeman spin Hamiltonian is

$$\mathcal{H}_Z = -\gamma\hbar\sum_i h_iS_i = -\frac{\gamma\hbar}{2}\begin{bmatrix}0 & h\\ h^* & 0\end{bmatrix},$$

where h_i is a random MF on the electron, for simplicity $h_z = 0$ is assumed, and $h \equiv h_x - {\rm i}h_y$ is denoted. We assume that $\langle h_i(t)\rangle = 0$ and $\langle h_i(t)h_k(t')\rangle = q_{\rm ze}\,\delta_{ik}\delta(t-t')$, where $q_{\rm ze} = \tau_{\rm c}\sigma_H^2$ is the spectral density of the random MF. Substituting the wave function $\Psi \equiv \binom{f}{g}$ in the Schrödinger equation $\partial_t\Psi = -({\rm i}/\hbar)\mathcal{H}_Z\Psi$ gives a system of equations for the components of Ψ, $\partial_t f = {\rm i}\gamma hg/2$ and $\partial_t g = {\rm i}\gamma h^*f/2$, whose solution with the initial conditions $f(0) = 1$, $g(0) = 0$ is $f(t) = \cos(W/2)$, $g(t) = {\rm i}\sin(W/2)$, where $W \equiv \gamma\int_0^t h(t')\,{\rm d}t'$ is a Brownian process. Hence, the quantum mechanical average of the z-projection of spin is $s(t) = (1/2)f^*f - (1/2)g^*g = (1/2)\cos[W(t)]$. This expression reproduces (17) where, instead of w, we must substitute γh and, accordingly, instead of (22), use the correlator

$$\left\langle\gamma\left[h_x(t_i) + {\rm i}h_y(t_i)\right]\gamma\left[h_x(t_j) - {\rm i}h_y(t_j)\right]\right\rangle = 2\gamma^2 q_{\rm ze}\delta(t_i-t_j) = \frac{q'}{2\hbar^2}\,\delta(t_i-t_j),$$

where we set $q' \equiv 4\tau_{\rm c}\gamma^2\hbar^2\sigma_H^2$. Then, the decoherence time via the Zeeman channel follows immediately from (25), where, instead of q, we must substitute q':

$$\tau_{\rm ze} = \frac{4\hbar^2}{q'} = \frac{1}{\tau_{\rm c}\gamma^2\sigma_H^2}. \qquad (28)$$

We note that a random MF can be caused by random vibrations of both a magnetic nucleus and another paramagnetic center, i.e., by the mechanism of magnetic dipole–dipole interaction.

SOI channel. Spin–orbit interaction is another known source of spin relaxation in liquids and solids. An atom is involved in thermal motion in the Coulomb field of the nucleus and neighboring atoms. Electron spin moves in an electric field (EF) and interacts with it, because SOI is proportional to the EF, spin, and electron momentum.

SOI arises in the nonrelativistic limit of the Dirac equation and leads to the fine splitting of atomic spectral lines; the hyperfine splitting is much smaller. The difference between the SOI and HFI scales in an atom is about three orders of magnitude. An illustration of HFI is provided by the interaction of magnetic moments of the electron and the nucleus, whereas SOI is the interaction of the electron magnetic moment with the MF arising in its own coordinate system when moving in the EF of the nucleus. Possible involvement of SOI in magnetic biological effects was discussed in [169, 170]. SOI provides spin decoherence due to its modulation by thermal fluctuations of the medium having a distributed dipole moment.

The SOI is described by an operator proportional to spin $\mathbf{S}$, the EF vector $\mathbf{E}$, and the electron momentum $\mathbf{p} = -i\hbar\nabla$ [171, p. 151]:

$$\mathcal{H}_{so} = -\frac{e\hbar}{2m^2c^2}\,\mathbf{S}[\mathbf{E}\times\mathbf{p}]\,.$$

Given the spherical symmetry of the nuclear EF, this operator reduces to the usual form of the product of spin and orbital moments of the electron. In condensed matter, the spherically symmetric field of the nucleus is perturbed by a random EF from neighboring dipoles undergoing thermal displacements, and therefore the SOI operator acquires a nonspherical random component causing decoherence of spin states.

To estimate the possible influence of a random EF on the decoherence time, we consider the simple case of one-dimensional electron motion along the z-axis in the EF $\mathbf{E}\perp\mathbf{z}$ and, for greater generality, in the MF H directed along the same axis. The SOI operator in the Zeeman basis can be written as

$$V = -\eta\begin{bmatrix} 0 & E_{xy} \\ E_{xy}^* & 0 \end{bmatrix} p_z\,, \quad \eta = \frac{e\hbar}{4m^2c^2}\,, \tag{29}$$

where $E_{xy} \equiv E_y(t) + iE_x(t)$, $e = |e|$ and m are the charge and mass of the electron, and c is the speed of light. As in the case of perturbation correlators (13) from the HFI section, we assume that $\langle E_i(t)\rangle = 0$ and $\langle E_i(t)E_j(t')\rangle = q_E\,\delta_{ij}\delta(t-t')$, where $q_E = \tau_c\sigma_E^2$ is the power spectral density of EF fluctuations. The equation of motion has the form

$$\partial_t\Psi = -\frac{i}{\hbar}\left[\mathcal{H}_0 + \mathcal{H}_Z + V(t)\right]\Psi\,,$$

$$\mathcal{H}_0 \equiv \frac{p_z^2}{2m}\,, \quad \mathcal{H}_Z \equiv -\varepsilon\sigma_z\,, \quad \varepsilon \equiv \frac{1}{2}\,\gamma\hbar H\,,$$

where $\mathcal{H}_0$ and $\mathcal{H}_Z$ are the respective free motion and Zeeman operators, and σ_z is the Pauli matrix. It can be shown that calculations analogous to those given above yield the decoherence time

$$\tau_{so} = \frac{4\hbar^2}{q'} = \frac{\hbar^2}{4\tau_c\eta^2p^2\sigma_E^2}\,. \tag{30}$$

The decoherence time in this scenario is independent of the constant MF, despite the presence of Zeeman interaction.

Decoherence time (30) decreases rapidly with increasing momentum p, or with increasing angular momentum if this result is applied to a real molecule. In molecules having axial symmetry, like the hydroxyl radical HȮ, the population of states with nonzero angular momentum can be significant even in liquid, which leads to a noticeable anisotropy of the g-factor and fast spin decoherence: it occurs in less than 1 ns [172].

Exchange interaction channel. In the context of magnetic biological effects, the exchange interaction of electrons of a radical pair is typically neglected. It is believed that by introducing additional mutual influence of spins, it reduces the possible magnetic effect. This happens due to the induction of additional singlet–triplet conversion, destroying the finely tuned 'symbiosis' of Zeeman and hyperfine interactions. Below, we show that the induction of singlet–triplet transitions by exchange interaction is not the only reason why exchange destroys magnetic effects. Random oscillations of exchange interaction also occur, and they themselves cause spin decoherence, being a general cause of suppression of magnetic RPM effects.

The exchange Hamiltonian of a pair of electrons is (see, e.g., [71, p. 289])

$$\mathcal{H} = -\hbar J(\mathbb{1}/2 + 2\mathbf{S}^1\mathbf{S}^2)\,,$$

where $\mathbb{1}$ is a four-row identity matrix and J is the magnitude of exchange interaction in frequency units, varying together with the randomly oscillating distance between electrons. Omitting the constant component for simplicity, we set $\langle J(t)\rangle = 0$ and $\langle J(t)J(t')\rangle = q_{ex}\,\delta(t-t')$, where $q_{ex} = \tau_c\sigma_J^2$ is the spectral density of random variations in the exchange interaction. Calculations analogous to those above show that the decoherence time via the exchange channel is

$$\tau_{ex} = \frac{4\hbar^2}{q''} = \frac{1}{2\tau_c\sigma_J^2}\,. \tag{31}$$

3.3 Estimates of decoherence time

Hyperfine interaction. The estimate of the decoherence time via the HFI channel, Eqn (25), is $\tau_{hf} = 4\hbar^2/\tau_c\sigma_v^2$. Because $v(t)$ in (13) is the variable component of HFI, equal by order of magnitude to the energy of dipole interaction of the electron magnetic moment and the moment $v \sim \mu_B\mu_N/r^3$ of the external magnetic nucleus located at a distance r, $\sigma_v^2 \sim \mu_B^2\mu_N^2\mathrm{D}[r^{-3}(t)]$, where D[...] denotes the variance, and μ_B and μ_N are Bohr and nuclear magnetons. We introduce a dimensionless distance $x \equiv r/r_B$. Then, $\mathrm{D}[r^{-3}(t)] = r_B^{-6}\mathrm{D}[x^{-3}(t)]$. Then, $\sigma_v^2 \sim \mu_B^2\,\mu_N^2 r_B^{-6}D$, where the dimensionless quantity D is $\mathrm{D}[x^{-3}(t)]$. Substituting all this into the formula for the decoherence time and setting $\tau_c \sim 100$ ps, we obtain $\tau_{hf} \sim D^{-1}4\hbar^2r_B^6/(\tau_c\,\mu_B^2\,\mu_N^2) = 0.45\times10^{-6}D^{-1}$ s. An estimate of D^{-1} is given below.

Let us clarify the choice $\tau_c \sim 100$ ps of the correlation time of thermal fluctuations of atomic groups surrounding the radical. The amplitude of thermal oscillations of atomic groups in proteins is much larger than the magnitude of oscillations of atoms in solids and liquids, because peptide bonds connecting amino acid residues allow rotations. Therefore, protein chains fold into globules and have much lower rigidity. Accordingly, the correlation time of perturbations grows, and it depends on many factors. In [173], the frequency range of vibrations of groups of atoms in a common protein was 0.4 THz, implying a correlation time of ~ 1 ps. In [140], by numerical simulation of the RPM with thermal rotational perturbations of a Trp radical, it was found that, for a noticeable orientational magnetic effect, the correlation time of rotational librations should be of the order of 100 ps. In [149], the correlation time of random displacements of a Trp radical was set equal to 1 ns. In [174], the rotational autocorrelation time of the flavin group in a protein was several nanoseconds, and in [175], the magnetic effect in the GMF with a radical lifetime of 1 μs was sufficiently large if the correlation time of random rotations exceeded 250 ns. We note that, for large times τ_c, comparable to the estimated value of τ, the approximation of delta-correlated perturbations becomes inapplicable. Given the above spread of times used, the compromise $\tau_c \sim 100$ ps appears reasonable.

Zeeman interaction. The decoherence time estimate via the Zeeman channel $\tau_{ze} = 1/(\tau_c\gamma^2\sigma_H^2)$ is similar to the estimate via the HFI channel, because both cases are about the influence of the MF fluctuations generated by random

oscillations of closely located magnetic dipoles. In this case, it is about the magnetic moment of a closely located paramagnetic ion or electron of the same radical pair: a moment creating an MF of the order of $H \sim \mu_B/r^3$ at distance r. This field is approximately 1800 times higher than that from a nuclear magneton, and therefore decoherence occurs approximately six to seven orders of magnitude faster. Indeed, $\sigma_H^2 \sim \mu_B^2 \mathrm{D}[r^{-3}(t)]$, or $\sigma_H^2 \sim \mu_B^2 r_B^{-6} \mathrm{D}[x^{-3}(t)]$ in terms of the dimensionless distance $x \equiv r/r_B$. Because we have set $D \equiv \mathrm{D}[x^{-3}(t)]$, we now have $\sigma_H^2 \sim \mu_B^2 r_B^{-6} D$. Accordingly, $\tau_{ze} \sim D^{-1} r_B^6/(\tau_c \gamma^2 \mu_B^2) = 8.2 \times 10^{-15} D^{-1}$ s.

To calculate τ_{ze}, we need to estimate the variance $D \equiv \mathrm{D}[x^{-3}(t)]$ based on some plausible distribution of the values of x. Recall that these are dimensionless distances, expressed in Bohr radii, between the radical electron and the source of perturbations. The normal distribution for x is not suitable, because it allows both negative and very large values, which makes no physical sense. Let the distribution of the values of x be constructed based on the β-distribution with the shape parameters $\alpha = \beta = 4$:

$$\mathrm{B}(x, r, \sigma) \equiv \frac{1}{2s} \,\mathrm{Beta}\left[\frac{x - r + s}{2s}, \alpha, \alpha\right], \quad s \equiv \sigma\sqrt{2\alpha + 1}\,. \quad (32)$$

The distribution is then symmetric with respect to the center r, and the shape approximates the normal distribution shape $\mathrm{N}(x, r, \sigma)$. Unlike the normal one, the distribution $\mathrm{B}(\ldots)$ under the nonbinding condition $\sigma < \mu/\sqrt{2\alpha + 1}$ has a bounded positive support $x \in [r - \sigma\sqrt{2\alpha + 1},\, r + \sigma\sqrt{2\alpha + 1}]$, which agrees with physics and is convenient for estimating variations in random quantities like $1/x^3$ and $\exp(x)$. With increasing α, the approximation accuracy increases, but the region of admissible values of σ narrows; therefore, a convenient compromise $\alpha = 4$ was chosen for estimates.

Using the laws of transformation of distributions under inversion, multiplication, and exponentiation and knowing the distribution of the values of x, we can find the distribution of the random quantity $1/x^3$,

$$\mathrm{C}(x, r, \sigma) = \frac{1}{6\, s\, x^{4/3}} \,\mathrm{Beta}\left[\frac{1}{2s}(x^{-1/3} - r + s), \alpha, \alpha\right],$$

with the support $[(r + s)^{-3}, (r - s)^{-3}]$. Hence, $D = \int (x - \langle x \rangle)^2 \mathrm{C}(x, r, \sigma)\, \mathrm{d}x$, where integration limits correspond to the support interval. The spin decoherence time $\tau_{ze} = 8.2 \times 10^{-15} D^{-1}$ s is plotted in Fig. 8 as a function of the distance r at several values of σ.

Evidently, the distance r cannot be less than $(2-3)\sigma$. We see that, if $\sigma = 0.1$ nm, then the decoherence time is of the order of 3 μs at $r = 1$ nm, but only 4 ns at $r = 0.5$ nm. If σ is twice as large, then this time is 300 ns at the distance 1 nm and 1 ns at the distance 0.7 nm. Of the two parameters, the distance r is decisive. The decoherence time drops rapidly, faster than the eighth power, as the distance between the radical electron and the dipole decreases and as the standard deviation of thermal oscillations of the dipole increases. Due to such a sharp dependence, reliable estimates can be obtained only from the exact dynamical structure of the environment of radical pairs.

Spin–orbit interaction. The decoherence time via the SOI channel, Eqn (30), is $\tau_{so} \sim \hbar^2/(4\tau_c \eta^2 p^2 \sigma_E^2)$, where $E(t)$ is the EF $E = d/r^3$ on the electron, created by an oscillating electric dipole d at a distance r, in the point dipole approximation. Then, $\sigma_E^2 \sim d^2 r_B^{-6} D$ and $\tau_{so} \sim D^{-1} \hbar^2 r_B^6/(4\tau_c \eta^2 p^2 d^2)$. Estimates of p and d are needed in what follows. The angular momentum of an electron in a p state in an atom is $\hbar$ by order of magnitude, whence the momentum estimate is $p \sim \hbar/r_B$. The dipole moments of amino acid residues are mainly from 1.5 to 3 D [176], and the dipole moments of simple molecules and common valence bonds in proteins are from approximately 0.5 to 3 D [177, pp. 9–59]; for a water molecule, 1.83 D. Recall that D is the unit of measurement of the electric dipole moment, equal to the moment of an electron at a distance of 1 Å. Water molecules can be present in active sites of enzymes where electron transfer processes occur, often accompanied by the emergence of intermediate radical pairs. For estimates, we take the dipole moment 1 D, i.e., $d \sim 2 r_B e$, where e is the absolute value of the electron charge. Using all these relations and estimates, as well as the value of η in (29) and the equality $\mu_B = e\hbar/(2mc)$, we obtain $\tau_{so} \sim D^{-1} \hbar^2 r_B^6/(16\tau_c\, \mu_B^4) = 2.1 \times 10^{-15} D^{-1}$ s.

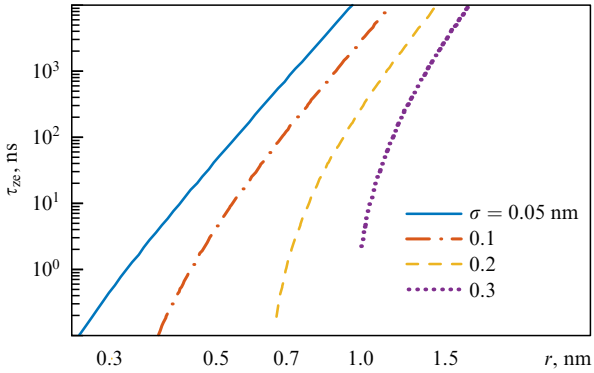

Figure 8. Dependence of time τ_{ze} of spin decoherence via Zeeman channel on average distance r to MF source at several values of standard deviation σ of random oscillations of r.

This decoherence time is the smallest of those considered above. However, it follows from (30) that, after pair creation, the electron must have a nonzero orbital moment (otherwise, the decoherence time is infinitely large). In view of the large size of flavin molecules and tryptophan amino acid residues forming electron radicals, and the involvement of processes of various natures in their photo or thermoionization, the appearance of uncompensated electrons in the s state with zero orbital moment and possibly with a slight admixture of states with $l \neq 0$ is most probable. In organic radicals, the anisotropy of the g-factor, arising when levels with nonzero l degenerate, differs little from the isotropic value [124]. The usual EPR linewidth of such radicals in proteins is of the order of 1 mT in an MF of several T, which suggests low anisotropy of the g-factor [178, p. 36], not more than 10^{-3}, which means an equally small relative population of states with nonzero l. By virtue of (30), this leads to an increase in the coherence time by many orders of magnitude. It is possible that, under the conditions just described, the SOI channel does not exceed the Zeeman one in efficiency of destroying coherence.

Exchange interaction. Exchange interaction of electrons, which is part of the Coulomb interaction, is determined by the overlap of their exponentially decaying wave functions. Such are, for example, radial functions of the ground state of the electron in a hydrogen atom. For a pair of hydrogen atoms, the overlap integral of wave functions centered at a distance r

decays rapidly, approximately as $\exp(-\varkappa r^{5/3})$, where $\varkappa$ is a constant. In a diamagnetic protein medium, the interaction of radical electrons decays more slowly: they are capable of tunneling through covalent and hydrogen bonds [179] to distances up to 3 nm [180]. Based on these data, the authors of [89] estimated the magnitude of the exchange interaction of flavin–tryptophan radicals in a cryptochrome protein depending on the interradical distance: $J(r) \sim J_0 \exp(-\varkappa r)$, $\varkappa \sim 14\ \text{nm}^{-1}$, $J_0 \sim 8 \times 10^{13}\ \mu\text{T}$. Then, knowing the variance of random changes of r, we can estimate the variance in the exchange interaction magnitude $\sigma_J^2(r, \sigma_r)$ and spin decoherence time (31): $\tau_{\text{ex}} = 1/(2\tau_c \sigma_J^2)$.

The amplitude of vibrations of a radical in CRY3 cryptochrome was estimated in [139] by the molecular dynamics method and was about 0.1 nm. If the distribution of the values of r is an approximation of the normal distribution $\text{N}(r, \sigma_r)$ by a shifted and scaled β-distribution $\text{B}(r, \sigma_r)$ (32), then, with fluctuations of r around the mean value of 1.9 nm (the distance between radicals of the final FAD–Trp pair) with the standard deviation $\sigma_r = 0.1$ nm, the deviation σ_J is 890 μT, or $1.6 \times 10^8\ \text{s}^{-1}$ in frequency units: $J(1.9\ \text{nm}) = 0.22\ \text{mT}$. Hence, the decoherence time $\tau_{\text{ex}} \sim 200$ ns. However, with somewhat larger random deviations at $\sigma_r = 0.15$ nm, the decoherence time drops to 10 ns.

The above estimates are unreliable due to the low fidelity in the constants J_0 and $\varkappa$ [90] and due to the strong dependence of σ_J on r and σ_r. For example, already with a 1% variation in r, the value of σ_J can change by tens of percent. Here, a significant role is more likely to be played by rare large fluctuations in r, when just one event of approach suffices for electrons to lose their spin coherence. Because amplitudes of displacements of atomic groups in proteins can be quite large, up to 1 nm [173], random approaches of the electron pair to distances of fractions of a nanometer are quite plausible. The possible role of such events in the RPM remains unexplored.

Thus, the spin decoherence time, which actually determines the emergence of a noticeable magnetic effect, depends quite strongly on the distance between electrons in the pair, such that its small variation can be a decisive factor for the existence of the magnetic effect. Under these conditions, theoretical estimates become unreliable, and it is reasonable to rely only on experimental data on magnetic effects directly dependent on τ. These data, even when they concern *in vitro* cryptochrome proteins [40] with an interradical distance up to 2–3 nm, show only insignificant effects at the level of 2% mT^{-1} and thereby testify to a spin decoherence time orders of magnitude smaller than a microsecond.

General remarks. It is worth bearing in mind that the true spin decoherence time can even be much less than the above estimates for several reasons. The decoherence time decreases as the inverse number of electric and magnetic dipoles surrounding the radical electron, because variances in their fields add up. In [98], the HFI of an electron pair, even with a few neighboring nuclei, entailed pseudorandom dynamics and hence rapid spin decoherence. In addition, both radicals of the pair experience spin decoherence independently, and therefore their mutual dephasing, which influences the magnetic effect, occurs about twice as fast.

Radical pairs arise not only in cryptochromes and photolyases but also in enzyme–substrate complexes because of an oxidation–reduction process accompanied by electron transfer in the active center of the enzyme [128]. For all the decoherence channels considered, there is a strong dependence of τ on the distance to the source of perturbations and the amplitude of its fluctuations. Because the arrangement of active sites of enzymes is such that it implies close contacts of the reacting peptides, amino acids, and proteins at a relatively low rate of actual chemical events, rapid spin decoherence in them looks plausible. The size of a radical pair arising in the active site of an enzyme can be significantly less than 2 nm. For example, for electrons at a distance of 1.2 nm with the vibration amplitude 0.01 nm, only exchange interaction with the parameters indicated in the preceding section would give a decoherence time of the order of 100 ps. The RPM effect, according to the relation $\gamma H \tau \sim 1$, could then be observed in an MF exceeding the GMF by more than 1000 times. This corresponds to the commonly used MF magnitudes for observing the RPM effects in enzymatic reactions *in vitro* (see, e.g., [15, 181]). We add that an increase in the spin decoherence rate occurs under the synergistic, simultaneous action of several decoherence channels.

In [100], the chemical reaction itself, represented by an operator, was proposed as another source of decoherence in the RPM. Identifying a discontinuous chemical process with a continuous quantum measurement is counterintuitive, although the idea of atomic energy exchange events as quantum collapses is not ungrounded [182; 183, p. 197]. This approach may give an extended interpretation of quantum RPM processes, but does not facilitate the acceptance of the hypothesis of slow spin relaxation in magnetically sensitive proteins. Notably, it was shown in [94] that accounting for this spin decoherence channel leads not to a decrease but to a two-fold increase in the rate of reduction of off-diagonal elements of the density matrix, and this means acceleration of relaxation of quantum coherence.

It is clear that, in any case, the hypothesis of microsecond and longer spin relaxation times in estimates of the RPM effects in proteins, which is often assumed by default to explain magnetic biological effects of a weak MF, is not substantiated. Estimates taking the *dynamic* structure of specific enzymes into account are needed, because X-ray crystallography gives the structure of proteins in their crystalline, not functional, state.

Thus, there are grounds to believe that, in the absence of an MF or in an MF less than the GMF, the spin decoherence time of radicals in protein media can be less than 10 ns in order of magnitude. In view of the absence of experimental facts confirming microsecond spin decoherence times of radical electrons in proteins and, conversely, the presence of facts consistent with the assumption of nanosecond times (at least in active centers of enzymes), it is reasonable to use the nanosecond range of τ in estimating expected nonspecific magnetic effects.

4. Discussion

4.1 Dependence of RPM effect on chemical kinetics and spin relaxation rates

The parameter s in (11) is $s \equiv k/g = \kappa\tau$. Judging by the totality of experimental data and estimates, realistic values of the relaxation time τ do not exceed 100 ns, and the rate of chemical kinetics of long-lived radicals in proteins is $\kappa \lesssim 1\ \mu\text{s}^{-1}$. We therefore assume that $s \lesssim 0.1$, and hence s is a small parameter. Then, the function $M_a(h, \theta, s) = h^2 s(\theta^2 - 1.25^2)/5$ is an approximation of (11) at $h < 0.1$

and $s < 0.1$, where $O(h^2 s^2)$ and $O(h^4 s)$ terms are neglected in the expansion of M. Nowhere in the range $1.25 \leqslant \theta \leqslant 10$, i.e., in region E of magnetobiological effects in Fig. 4a, does this function deviate from (11) by more than 4% on a logarithmic scale. For convenience, we present its fully dimensional form using notation (3),

$$M_{\rm a}(H,\kappa,\tau) = \frac{1}{5}\,\gamma^2 H^2 \kappa\tau \left[\frac{\tau^2}{(1+\kappa\tau)^2} - \frac{1{,}25^2}{a^2}\right], \qquad (33)$$

where a is the isotropic HFI constant and all quantities are expressed in the Gaussian system. The applicability range of formula (33) in terms of the MF magnitude is $H \lesssim H_{\rm geo}$. Another constraint is on the values of kinetic and relaxation rates, $\kappa\tau \lesssim 0.1$ and $\kappa + 1/\tau < a/1.25$; in this region, the expansion is valid and the magnetic effect in Eqn (33) remains positive. Figure 9a shows the dependence of $M_{\rm a}(H,\kappa,\tau)$ on τ at several values of κ. Good correspondence between the original function and its approximation can be seen. The magnitude of the RPM effect decreases approximately as τ^3 with decreasing τ. If we focus on the accuracy of approximating the largest (at the level of 10^{-3}–10^{-2}) of these small effects, then an even simpler relation $M_{\rm ar} \approx 0.2(\gamma H\tau)^2\kappa\tau/(1+\kappa\tau)^4$ can be used (Fig. 9b).

An effect quadratic in H in the range of low MFs up to 1 mT was observed experimentally, e.g., in [61, 184–188] and estimated theoretically, e.g., in [153, 189–191]. An analytic dependence of the RPM effect on the spin decoherence time τ had not been proposed previously; here, it is obtained in form (11) and (33).

4.2 Hypomagnetic field effect

Recently, attention to biological effects of the hypomagnetic field (hypoMF), more precisely, to effects initiated by the suppression of the natural GMF by one to two or more orders of magnitude, has been growing. The interest is not unreasonable: in a zero MF, qualitative changes occur in the quantum dynamics of the magnetic moments of *all* microparticles that have magnetic moments. In a zero field, there are more chances to observe difficult-to-reproduce magnetic biological phenomena.

Organisms on Earth have evolved in the GMF, and hence its absence can cause disturbances in the normal functioning of organisms. Suppression of the GMF in laboratory conditions is accompanied by changes in biochemical indicators and behavior of a wide variety of organisms: from bacteria and fungi to mammals and humans (see, e.g., [55, 192, 193]). In deep space flight and in future missions to the Moon and Mars, astronauts will be in hypoMF conditions. This is associated with additional risk. The action on organisms of MFs weakened compared to the GMF is an area of space medicine [194].

It is convenient to define the hypomagnetic effect such that it equals zero in the GMF and unity in a zero MF. Then, assuming it to be caused by the RPM process, it follows immediately from (33) that $M_{\rm hypo} = 1 - (H/H_{\rm geo})^2$, where $H_{\rm geo}$ is the GMF magnitude (Fig. 9c). This relative effect makes sense when the absolute effect is sufficiently large compared to the natural spread of biological variables. $M_{\rm hypo}$, like M, represents only changes in the integral components of the density matrix of a radical pair. Due to further nonlinear signal transduction to the observational level, experimental MF dependences can differ significantly.

Thus, the magnetic effect in Eqn (33) decreases as H^2 with decreasing MF, and very rapidly, as τ^3, with decreasing relaxation time, while remaining insignificant in the entire range of variable changes. Consequently, it is quite difficult to explain the observed magnetic nonspecific effects in biology, sometimes exceeding tens of percent, based on the RPM in its canonical form, without assuming additional amplification of primary RPM signals.

4.3 Influence of radiofrequency magnetic fields

For experimental proof of the involvement of a quantum chemical RPM compass in animal magnetic navigation, a high-frequency MF supplementary to the GMF, covering the animals' dwelling space [195–199], or the field of a small emitter attached to an animal's head [197, 200], was used. It was assumed that an MF with a nearly resonance frequency would cause quantum transitions in the Zeeman states of radical pairs in retinal cryptochromes, which would disrupt the RPM operation and thus confirm its involvement in magnetoreception. There is a similarity with one of the methods for detecting magnetic resonance, namely, by the reaction yield (RYDMR) [201, 202]. In the case of the RPM in biology, however, resonance should manifest itself in a change to a biological variable.

In estimating this effect, the amplitude of the additional MF and the spin decoherence time are important, in addition to the frequency. In [157], the RF MF contribution to the magnetic RPM effect was investigated based on the Liouville–von Neumann equation (4) with the Zeeman Hamilto-

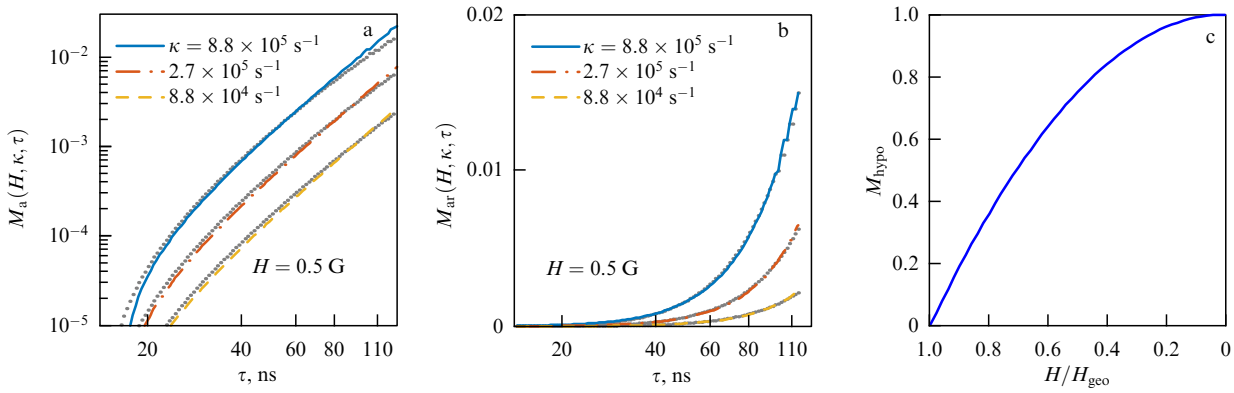

Figure 9. (a) Dependence of $M_{\rm a}(H,\kappa,\tau)$ on τ at several values of κ, calculated by formula (33). Dashed line shows calculation with same parameter values using formula (11) for M. (b) Same using formula for $M_{\rm ar}$. (c) Hypomagnetic effect, relative effect when reducing MF from GMF to zero.

nian and using notation (3). The MF was directed along the z-axis and included a perpendicular variable component, $\mathbf{H} \equiv h[\varepsilon\cos(\omega t), \varepsilon\sin(\omega t), 1]$, where ε and ω are the relative amplitude and frequency. The relative magnetic effect in a variable MF in such a system was obtained in the form of a Lorenzian resonance contour,

$$\tilde{M}(h,\varepsilon,\omega,g) = \frac{\varepsilon^2 h^2}{g^2 + \varepsilon^2 h^2 + (\omega - h)^2},$$

with a width of the order of $\sqrt{g^2 + \varepsilon^2 h^2}$. In a low field $\varepsilon \ll 1$, the resonance width is g or, by virtue of (3), $1/\tau$ in units of s^{-1}, which is a well-known result (see, e.g., [111; 203, p. 15]). It has been shown that, even under conditions favoring the observation of the magnetic resonance effect, at exact resonance in a two-level system in the absence of the chemical kinetics and interactions other than Zeeman, the variations introduced into the population of quantum levels of such an idealized system under perturbations as in the aforementioned experiments are insignificant, less than 10^{-5}, and cannot disrupt the RPM regularities. This estimate was obtained at a large spin relaxation time of 1 μs ($g \approx 0.01$). At plausible decoherence times of 3–30 ns in proteins, the effects of the RF MF in the indicated experiments are vanishingly small.

Interestingly, the conclusion about the absence of the influence of small RF fields on the RPM effect was made in [50] based on numerical calculations even in the absence of both kinetics and spin decoherence. Even earlier, in terms of Bloch relaxation times $T_{1,2}$, it was shown that explaining the observed influence of RF MFs on the magnetic orientation of animals within the EPR theory would require an impossible electron spin relaxation time of 1 s [204].

Thus, the disruption of the magnetic orientation ability of animals in very small variable MFs observed in all the abovecited experiments is hardly related to the RPM. This connection would be possible only assuming some further amplification of such a small primary RPM signal, and only if this primary signal reached values of 10^{-4}–10^{-3} typical of the RPM. Also unstudied remains the possible influence on the orientation ability from the electric component of the RF field.

4.4 Is quantum entanglement needed in RPM?

Currently, considerable attention is drawn to the fundamental property of composite quantum systems to be in so-called entangled states, when there is an inexplicable correlation of system parts [205]. This property, underlying the famous EPR paradox [206], finds application in quantum cryptography, quantum computing, and quantum microscopy [207–211].

It has been proposed that the resource of quantum entanglement previously unaccounted for in magnetobiology could resolve RPM contradictions. Whether the entanglement of the initial state is a significant factor in explaining RPM effects is discussed in [33]. The authors argue that it is not, however indirectly, without quantitative calculation of the entanglement of mixed states. In [97], the entanglement of the evolving density matrix in the RPM model was quantitatively estimated, but the connection of the initial state entanglement with the RPM effect was not discussed. In [35], the evolution of entanglement of the electron–nucleus system relative to the electron-singlet initial state was investigated, although in a simplified RPM model without accounting for thermal relaxation or the chemical kinetics. Different measures of entanglement in relation to the RPM were considered in [34, 101, 212].

Below, a quantitative estimate of entanglement is performed and correlations between purity and entanglement of the initial state, on the one hand, and the magnitude of the emerging magnetic effect, on the other, are presented in the RPM model with spin relaxation and chemical kinetics.

An entangled state of a composite system, unlike an unentangled, or separable, one, does not allow writing the wave function of the system as a product of wave functions of the parts (see, e.g., [76, p. 80]). There is no single measure of the entanglement of quantum states of systems, because entanglement is a phenomenon with a variety of properties [213]. Accordingly, different measures of entanglement have been proposed for both pure and mixed states [214, 215]. We recall that a pure state is a superposition of eigenstates, and the density matrix of a mixed state is a linear combination of density matrices of pure states with weights given by probabilities.

Entanglement of quantum states is determined, in particular, based on the von Neumann entropy, $-\operatorname{tr}(\rho\ln\rho)$, which is a positive quantity equal to zero for separable states. Entanglement of pure states of a composite system is then the entropy of any of its parts (see, e.g., [215]). For mixed states, a unified definition does not exist. If we are talking about pure states of a system AB, i.e., about the state vector of the system, then entanglement is defined via the negation of separability, which in this case reduces to the possibility of representing the system state as a tensor product of state vectors of parts A and B. If we are talking about mixed states, representable only by a density matrix, then the definition of entanglement becomes more complicated. In that case, the system state is considered entangled [216] if its density matrix is not representable as a combination of possible tensor products of density matrices of the parts, i.e., in the form $\rho_{AB} = \sum_i p_i \rho_A^i \otimes \rho_B^i$, with $\sum p_i = 1$. This more general definition of separability links it to the possibility of factoring not the unobservable density matrix but the expectation values of measurement results of observables in parts A and B. The number of sum terms is limited by the square of the dimension of the Hilbert space of the system [214].

In [217], the relative entropy of entanglement was proposed as a measure of entanglement of a mixed state. This is the minimum distance from the entangled state ρ to a separable one ρ', the minimum taken on the subset of separable states ρ'. The relative von Neumann entropy $S_{\text{rel}}(\rho|\rho') \equiv \operatorname{tr}(\rho\ln\rho - \rho\ln\rho')$ is used as the distance. If the density matrices are representable as spectral decompositions with respect to projectors onto eigenstates, $\rho = \sum_i r_i |i\rangle\langle i|$ and $\rho' = \sum_j s_j |j\rangle\langle j|$, then the relative entanglement entropy is [218, p. 109]

$$S_{\text{rel}}(\rho|\rho') = \sum_i r_i \left[\ln r_i - \sum_j P_{ij}\ln s_j\right], \quad P_{ij} \equiv \langle i|j\rangle\langle j|i\rangle, \tag{34}$$

where it is assumed $0\ln 0 \equiv 0$. We always have $S_{\text{rel}} \geqslant 0$; it is seen that $S_{\text{rel}} = 0$ at $\rho = \rho'$. Measure (34) is used to calculate entanglement in what follows.

Equation (5) describes the evolution of a composite system that includes a pair of electrons and a magnetic nucleus. Because it was assumed that the initial state of electrons is always singlet, the spins of the electron pair are one part of the system, and the spin of the magnetic nucleus is

the other part. Then, generally speaking, the initial matrix ρ_0 of the system of electron spins and the nuclear spin in an arbitrary state can be constructed in different ways. The above choice $\rho_0 = P/\operatorname{tr}(P)$, where P is the projector onto the singlet state (which is antisymmetric and has zero total electron spin), corresponds to a completely undefined state of the nuclear spin. However, the magnetic effect in the considered RPM model depends on what state the nuclear spin was in at the initial moment of time: the singlet state of the electron pair is antisymmetric under their permutation, but only the first electron experiences the action of the hyperfine field of the nucleus.

Let $|\sigma_\uparrow\rangle \equiv |\sigma\rangle \otimes |\uparrow\rangle$ and $|\sigma_\downarrow\rangle \equiv |\sigma\rangle \otimes |\downarrow\rangle$ be the states of the system corresponding to the singlet state of electrons $|\sigma\rangle$ and different projections of the nuclear spin. These are separable states because they are products of spin functions of the parts. The initial density matrix used in calculating (7) in this notation has the form $\rho_0 = |\sigma_\uparrow\rangle\langle\sigma_\uparrow|/2 + |\sigma_\downarrow\rangle\langle\sigma_\downarrow|/2$, which corresponds to the maximally mixed state of the system, also maximally entangled in nuclear spin states. But the initial state of the nuclear spin is unknown, and the magnetic effect could depend on both purity and entanglement of ρ_0.

The density matrix of the initial state in the general form of various degrees of purity and entanglement is constructed as follows. We first write the normalized state $\psi(b,\phi) = b|\sigma_\uparrow\rangle + \exp(\mathrm{i}\phi)\sqrt{1-b^2}|\sigma_\downarrow\rangle$ of a pure superposition of separable states $|\sigma_\uparrow\rangle$ and $|\sigma_\downarrow\rangle$, where the domains of real parameters are $b \in [0, 1]$ and $\phi \in [0, 2\pi)$. This is a pure entangled state. Its density matrix is $\rho_{\mathrm{pur}}(b,\phi) = \psi(b,\phi)\psi^+(b,\phi)$. We now create a density matrix of an arbitrary mixture of such pure states,

$$\rho_{\mathrm{mix}}(a, b_1, \phi_1, b_2, \phi_2) = a\rho_{\mathrm{pur}}(b_1, \phi_1) + (1-a)\rho_{\mathrm{pur}}(b_2, \phi_2)\,, \tag{35}$$

where $a \in [0, 1]$ is a real constant. This is a general-form density matrix of an electron-singlet state with arbitrary purity and entanglement relative to the nuclear spin, depending on five parameters.

It is not difficult to find that the purity of this state, defined by the trace of the square of the density matrix, $\mathrm{pur} \equiv \operatorname{tr}(\rho_{\mathrm{mix}}^2)$, ranges from 1/2 to 1; the value 1 corresponds to a pure state,

$$\mathrm{pur}\,(a, b_1, \phi_1, b_2, \phi_2) = 1 - 2a(1-a)\Big[b_1^2 - 2b_1^2 b_2^2 + b_2^2 - 2b_1 b_2\sqrt{1-b_1^2}\sqrt{1-b_2^2}\,\cos(\phi_1 - \phi_2)\Big]\,. \tag{36}$$

A pure state, as can be seen from (35) and (36), occurs when $a = 0$ or $a = 1$, or if $b_1 = b_2$ and $\phi_1 = \phi_2$ simultaneously. The estimate of the entanglement $E(\rho_{\mathrm{mix}})$, as stated above, is found from relative entropy (34) by minimizing it on the set of separable states:

$$E(\rho_{\mathrm{mix}}) \equiv \min_{\{\rho_{\mathrm{sep}}\}} S_{\mathrm{rel}}(\rho_{\mathrm{mix}}|\rho_{\mathrm{sep}})\,. \tag{37}$$

The density matrix of any separable initial state ρ_{sep} differs from ρ_{mix}. It is a tensor product $\rho_{\mathrm{sep}} \equiv \rho_{\mathrm{e}} \otimes \rho_{\mathrm{n}}$, where $\rho_{\mathrm{e}} \equiv |\sigma\rangle\langle\sigma|$ is the density matrix of the electron pair state that is singlet by assumption, and ρ_{n} is the density matrix of the general form of a mixed nuclear-spin state. The latter is constructed from a mixture of superpositions of nuclear spin eigenstates $\xi(b,\phi) = b|\uparrow\rangle + \exp(\mathrm{i}\phi)\sqrt{1-b^2}\,|\downarrow\rangle$; setting $\rho_\xi(b,\phi) \equiv \xi(b,\phi)\xi^+(b,\phi)$, we obtain

$$\rho_{\mathrm{sep}}(a, b_1, \phi_1, b_2, \phi_2) \equiv \rho_{\mathrm{e}} \otimes \big[a\rho_\xi(b_1, \phi_1) + (1-a)\rho_\xi(b_2, \phi_2)\big],$$

where the same notation is used for the parameters as in the foregoing. Finally, from different matrices ρ_{sep} (the 64 of them in our case), their convex combination with random coefficients is constructed. This gives a separable state ρ_{sep} in the general form used for calculations in (37). Because the matrices ρ_{mix} and ρ_{sep} are cumbersome, we do not present them here.

By varying the parameters of the separable state matrix, we can numerically determine the entanglement of each specific matrix ρ_{mix}. By choosing the ρ_{mix} parameter values randomly, 5000 initial density matrices $\rho_0 \leftarrow \rho_{\mathrm{mix}}$ were generated, their purity (36) and entanglement (37) were determined, and magnitudes of the corresponding magnetic effects were calculated (numerically, because formula (11) is derived for ρ_0 maximally mixed with respect to nuclear spin). Is there a correlation between them?

Figure 10 shows the calculation results. We can see that all quantities correlate. It is also seen that purity and entanglement, although correlated, are independent characteristics of the quantum state. A negative correlation, −0.5, exists between entanglement and the magnitude of the RPM effect. Maximum effects can appear at pure initial states with intermediate entanglement 1/4.

The growth of electron–nucleus entanglement is accompanied on average by a decrease in the effect. However, this is only a correlation. It would be difficult to speak of a dependence of the magnetic effect on entanglement. Entanglement is a complex nonlinear function of the quantum state, parameterized by several parameters, but the converse is not true: a quantum state is not a function of entanglement. For a given entanglement magnitude, the state of the system is not defined, even if the purity is also known. Knowing E, it is impossible to calculate the state parameters, which would be necessary to calculate the RPM effect. Here, entanglement is merely an epiphenomenon of the magnetic effect, unlike the field of quantum computing, where it can be controlled and where it is a useful resource. Thus, the question posed in the section title can be answered unequivocally. Quantum entanglement is not a useful factor in studying RPM effects. What is important is ordinary quantum coherence, ensuring coordinated spin dynamics, and hence the magnetic effect.

The role of entanglement of the initial *electron* state was discussed in [159]. Here, it is chosen as a singlet, i.e., maximally entangled state $\rho_{\mathrm{e}} \equiv |\sigma\rangle\langle\sigma|$. We additionally solved Eqn (5) numerically with different combinations of electron-triplet initial states. The magnitude of the RPM effect indeed depends on state parameters up to the sign reversal of the effect; however, nothing qualitatively new compared to the case of a singlet state was found. In [212], the influence of the entanglement of a triplet initial electron state on the sensitivity of a chemical compass was studied, and it was found that entanglement is not a useful concept.

Another aspect of quantum coherence in RPM, the quantum Zeno effect, is also discussed in the literature. The effect arises when a quantum system starts from one of the eigenstates of some operator of an observable physical quantity. Periodic measurements of this quantity interrupt the unitary evolution of the system and return it to the nearest eigenstate, i.e., the initial one, with a high probability. If measurements are performed frequently enough, unitary

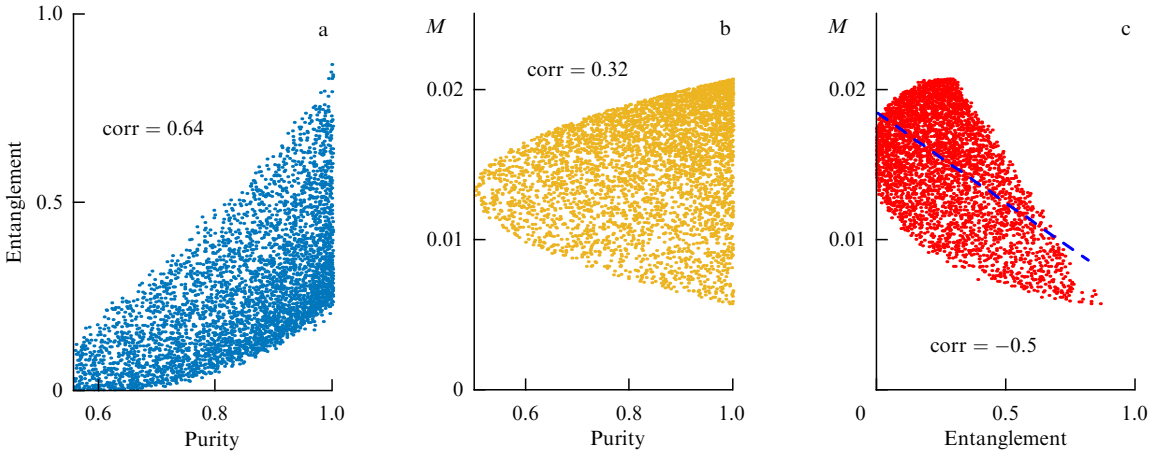

Figure 10. Correlations (a) between purity and entanglement of initial density matrix, (b) between purity and magnitude of magnetic RPM effect at $h = 0.1$, $g = 0.1$, and $k = 0.01$, and (c) between entanglement and magnetic effect magnitude. Values of correlation coefficient and linear regression are shown by dashed line for diagram (c).

evolution apparently 'freezes.' Regarding the RPM, the quantum Zeno effect is considered under the assumption that the chemical reaction has properties of a continuous quantum measurement causing decoherence. With such an approach, the form of the operator $-(1/2)\{kP + k'P', \rho\}$ of the chemical reaction in the Liouville–von Neumann equation [100] changes, but this does not change the magnitude of the RPM effect, which remains very small even at the microsecond scale of relevant characteristic times. The decoherence rate also changes little [94]. The authors of [151] show that the Zeno effect takes place with the standard chemical reaction operator as well, and its modification is not justified. As shown in [157], at realistic parameter values of the RPM model, the Zeno effect is impossible. Moreover, the Zeno effect consists in freezing quantum evolution, and the ST transitions in particular. But this contradicts the RPM, for which precisely the ST evolution is a necessary condition for operability. On the whole, this topic is insignificant for solving the physical problem of magnetic biology.

4.5 Are there competing mechanisms?

If we assume the spin decoherence time to be large, of the order of 1 μs, i.e., $g \sim k \sim 0.01$, then $\theta \sim 50$ and $s \sim 1$, which in the GMF $h = 0.1$, according to (10), gives a relative effect $M \sim 25\%$. This looks sufficient for the operation of a chemical quantum compass and, consequently, for explaining the magnetic orientation ability of animals. However, if the MF changes by 100 nT, i.e., $\Delta h \sim 2 \times 10^{-3}$, then M changes by only 0.1%. This means that, even with an implausibly large spin decoherence time, the RPM is unable to explain the specific sensitivity of some seasonally migrating species possessing special magnetoreceptors to geomagnetic variations in the MF at the level of tens of nT. There is also no explanation for multiple observed biological effects of geomagnetic disturbances on humans and other organisms (see, e.g., [219–222]). At plausible decoherence times of 3–30 ns, the effect does not exceed fractions of a percent in the GMF either. It seems that the smallness of the primary RPM effect M in (10) could be compensated by a subsequent amplification process. For example, such a process in the form of biopolymer ribosomal protein translation was proposed in [223]. The sensitivity can be enhanced by two to three orders of magnitude by including spin-correlated radical pairs in the work of biopolymer enzymes, in particular, ribosomal ones. In this case, the primary MF signal is converted into an increase in the number of incorrectly folded nonfunctional and often toxic protein globules, which creates an additional load on the protective functions of the organism and affects the speed and accuracy of cognitive processes. However, M in (10) is an abstract quantity introduced for the convenience of analysis. The real physical variable is the integral reaction product $1 - M$, which is a relative quantity equal to unity in the absence of an MF and almost constant in the GMF. Obviously, signal amplification in such a form makes no sense, because the resulting relative effect remains small.

Dissatisfaction with the markedly low responsiveness of the RPM to weak MFs is accompanied by a search for other mechanisms that would be more sensitive. We note immediately that many proposed mechanisms — those based on the Lorentz force, cyclotron, parametric, and magnetic resonances, magnetic induction, direct action of the MF on highly reactive molecules, etc. — are only of historical interest today [224]. In particular, unlike the triplet ground state of molecular oxygen, its singlet lowest-energy form, called singlet oxygen, has a high reactivity and can damage biopolymers. For this reason, it was sometimes assumed that the MF could influence the organism by directly exciting singlet–triplet transitions and increasing the concentration of singlet oxygen. However, the energy difference of singlet and triplet states of the O_2 molecule is many orders of magnitude larger than that of a radical pair in proteins, and hence a weak MF exerts no direct influence on singlet oxygen.

The response of organisms to the MF generally implies its necessary action on magnetic moments of atoms and molecules. Therefore, mechanisms have been developed for the MF influence on abstract single magnetic moments [225], on induced magnetic moments during the rotation of molecular groups inside biophysical structures [55, 226], and on nuclear magnetic moments [227, 228].

4.5.1 Single magnetic moment. Besides specific effects of magnetoreception, nonspecific effects exist, the epiphenomenon of life activity in the GMF. Their properties include sensitivity to MF reversal and frequency selectivity. The RPM does not explain such properties. Many studies show

the incompatibility of the observed effects with the RPM scenario [197]. For example, magnetic response arises under excitation by red light, which is insufficient for generating radical pairs, or in the dark [229]. Another mechanism is required to explain this. A separate MF sensor must react to the MF sign reversal. The insensitivity of the RPM to reversal follows from the influence of the MF on the *mutual* dynamics of a pair of moments. Therefore, a scenario where the MF alters the dynamics of a single moment with respect to a locally distinguished direction is promising [55, 230].

This mechanism is universal: its conclusions are independent of the nature of magnetic moments. It requires a minimum of variables and parameters, qualitatively explains nonspecific effects, and offers a method of experimental verification [225]. As shown in Section 1.3, the parameter $\gamma H\tau$, among other influence factors, controls the probability of sensor reaction to the MF. The value of H in the inflection region found in experiment is related to $\gamma\tau$, which allows clarifying the nature of the MF target (electron, proton, nucleus, or orbital moment), because their γs, as well as τs, differ considerably.

Importantly, some MF sensors are located on rotating molecules [230]. Calculations show that the response to the MF is shifted relative to a zero MF: $\gamma\tau(H - \Lambda/\gamma) \sim 1$, where Λ is the rotation speed. The effect changes under MF reversal, which allows distinguishing this mechanism from the RPM. The authors of experiments in [53, 229] interpret their results based on single moment dynamics, casting doubt on the explanation based on the RPM.

4.5.2 Mesoscopic quantum rotator. The action of the MF on organisms is possible only as the action on magnetic moments of atoms and molecules. However, the moment does not necessarily have to be a spin one. Rotation of charges leads to the emergence of a magnetic moment interacting with the external MF. A mechanism of biological effects of a weak MF was proposed based on the rotational motion of a molecule as a whole between two 'supports' in the form of covalent bonds with the nearest molecular framework [51, p. 385]. Despite thermal noise and a chaotic environment inside a living cell, the molecular rotator, thanks to increased inertia and immunity to support vibrations, has a relatively large decoherence time, which allows it to be in quantum superposition states and demonstrate quantum interference effects. This is just the mesoscopic region where quantum behavior clashes with classical. The gyromagnetic ratio of a molecular rotator is several orders of magnitude smaller than the electronic one due to the large mass of the gyroscope, but the coherence relaxation time is larger than the electronic one by the same several orders of magnitude [226]. Therefore, the fundamental relation $\gamma H\tau \sim 1$ governing the emergence of magnetic effects could be satisfied here.

The MF, influencing the phases of quantum states, affects interference and thereby changes the probabilities of the molecular group being in different angular positions. For example, a change in the probability of angular positions of amino acid residues during ribosomal translation or in the process of protein chain folding could affect the rate or results of protein synthesis. In active sites of DNA polymerases, steric restrictions could be weakened and allow almost free rotation of nitrogenous bases fastening DNA strands into a double helix. Interestingly, small-scale interference of the rotator is very sensitive to weak, but not to strong, magnetic fields. In addition, unlike the spin–chemical RPM, the quantum mesoscopic rotator demonstrates larger effects in a wide range of realistic values of the decoherence rate [55].

On the whole, it seems promising to search for such small-signal detection mechanisms that would be connected with comparative and highly nonlinear processes. Small signal variations in the background of a relatively large constant component could then turn into significant changes. Perhaps, the standard RPM and other models should be extended by combining them with kinetic schemes allowing positive feedback, as in 'error catastrophe,' for example [231]. Another prospect is associated with investigating not the average values studied in existing models of magnetic response but probabilities and effects of relatively rare but large fluctuations of quantum variables.

5. Conclusions

The available observational and theoretical information convincingly shows that the action of magnetic fields, even very small variations in the GMF, on organisms is a real state of affairs that must be reckoned with in biological and medical research and applications.

The spin–chemical RPM is regarded today as one of the most probable molecular mechanisms underlying the observed effects. In nonspecific RPM effects of a biological response to a weak MF, the primary targets of the MF are spin-correlated radical pairs with a typical thermal spin relaxation time of less than 100 ns. In this review, experimental and theoretical information available in the literature on the relaxation rate is presented, and simple estimates of the spin decoherence time τ of an electronic organic radical in a protein via hyperfine, Zeeman, spin–orbit, and exchange interaction mechanisms are given. All these data testify to the fact that the frequently used assumption of the radical electron decoherence times in proteins exceeding 1 μs is not substantiated. However, such an assumption is often used to align theory with experimental data on the magnitude of magnetic biological effects.

The magnitude of the RPM effects depends on the spin relaxation rate, but an explicit functional dependence has not been proposed until now. An analytic solution of the Liouville–von Neumann equation for a system of two electrons and a nucleus taking spin relaxation and chemical kinetics into account has been presented. The analytic solution is verified by numerical RK integration in a logarithmically wide range of relevant parameter values. It is shown that rates of chemical kinetics k and spin coherence relaxation g are combined into the parameters $k + g$ and k/g that respectively determine the shape and magnitude of magnetic effects. A simple approximating relation (33) has been found, applicable in the region of the most relevant parameter values of the RPM model. With a decrease in the spin relaxation time, the magnetic RPM effect decreases sharply as τ^3. Therefore, primary chemical RPM effects, occurring in the biochemical machinery of all organisms one way or another, are very small, of the order of 10^{-3}–10^{-4} or less. Magnetic RPM effects can acquire a noticeable magnitude only if the fundamental relation $\gamma H\tau \sim 1$, 'built in to' the RPM and consistent with the bulk of spin chemistry experiments, is satisfied.

Different aspects of relation (33) have been discussed: the influence of RF and hypomagnetic fields on magnetic navigation, the role of quantum entanglement of the initial state, etc. It is shown that the greatest influence on the

magnetic effect magnitude in a protein should be associated with conformational dynamics and thermal fluctuations of exchange interaction, leading to suppression of the effect to very small relative values.

Thus, at realistic spin decoherence rates, the calculated effects are small and cannot explain the observations. Despite increased theoretical understanding, the problem of magnetobiology still does not have a conceptual solution free from physical and methodological contradictions.

The immediate task in this field is apparently the measurement of the spin decoherence time of radicals in proteins *in vitro*. Important information about the nature of magnetic biological effects could be provided by measuring the dependences of the magnetic response on the hypomagnetic field on a logarithmic scale. The determination of the type of proteins initiating the magnetic response will likely happen within the next decade. The role of biopolymerization processes distinguishing living systems, in which large magnetic effects are observed, from *in vitro* systems, where the observed effects are small — processes possibly responsible for the amplification of insignificant primary magnetic signals — will be clarified.

The accumulated evidence of theoretical studies of the RPM and other models of magnetic response of organisms allows hoping for a speedy solution to the problem of magnetobiology. We have come closer to identifying the primary molecular target of the MF, and this opens the way to developing technologies for the directed action of weak electromagnetic fields on protein production in organisms and to the emergence of innovative medical methods.

References

1. Fleming G R, Scholes G D, in *Quantum Effects in Biology* (Eds M Mohseni et al.) (Cambridge: Cambridge Univ. Press, 2014) p. 3, DOI:10.1017/CBO9780511863189.003
2. Fraikin G Ya, Rubin A B, in *Gorizonty Biofiziki* (Horizons of Biophysics) Vol. 1 (Ed. A B Rubin) (Izhevsk: Inst. Komp'yut. Issled., 2022) p. 426
3. Asano M et al. *Quantum Adaptivity in Biology*: *From Genetics to Cognition* (Dordrecht: Springer, 2015) DOI:10.1007/978-94-017-9819-8
4. Menskii M B *Phys. Usp.* **48** 389 (2005); *Usp. Fiz. Nauk* **175** 413 (2005)
5. Ivanitskii G R *Phys. Usp.* **53** 327 (2010); *Usp. Fiz. Nauk* **180** 337 (2010)
6. Binhi V N *Fizicheskie Effekty Soznaniya*: *Zakon Vosproizvodimosti* (Physical Effects of Consciousness: the Law of Reproducibility) (Moscow: INFRA-M, 2021)
7. Khrennikov A Y *Open Quantum Systems in Biology, Cognitive and Social Sciences* (Cham: Springer, 2023) DOI:10.1007/978-3-031-29024-4
8. Ball P *Nature* **474** 272 (2011)
9. McFadden J, Al-Khalili J *Proc. R. Soc. London A* **474** 20180674 (2018)
10. Marais A et al. *J. R. Soc. Interface* **15** 20180640 (2018)
11. Syurakshin A V, Saleev V A, Yushankhai V Yu *Vestn. Samarskogo Univ. Estestvennonauchn. Ser.* **28** (1–2) 74 (2022) DOI:10.18287/2541-7525-2022-28-1-2-74-94
12. Barnothy M F (Ed.) *Biological Effects of Magnetic Fields* (New York: Plenum Press, 1964) DOI:10.1007/978-1-4899-6578-3
13. Grissom C B *Chem. Rev.* **95** (1) 3 (1995)
14. Binhi V N *Printsipy Elektromagnitnoi Biofiziki* (Principles of Electromagnetic Biophysics) (Moscow: Fizmatlit, 2011)
15. Buchachenko A L *Russ. Chem. Rev.* **83** (1) 1 (2014); *Usp. Khim.* **83** (1) 1 (2014)
16. Greenebaum B, Barnes F (Eds) *Biological and Medical Aspects of Electromagnetic Fields* Vols. 1, 2, 4th ed. (Boca Raton, FL: CRC Press, 2019) DOI:10.1201/9781315186641
17. Ghodbane S et al. *BioMed Res. Int.* **2013** 602987 (2013)
18. *Non-Ionizing Radiation* Pt. 1 *Static and Extremely Low-Frequency* (*ELF*) *Electric and Magnetic Fields* (IARC Monographs on the Evaluation of Carcinogenic Risks to Humans, Vol. 80) (Lyon: IARC Press, 2002)
19. Sarimov R M, Binhi V *Bioelectromagnetics* **41** 360 (2020)
20. Buchachenko A L, Kuznetsov D A *Russ. J. Phys. Chem. B* **15** 1 (2021)
21. Kirschvink J L, Jones D S, MacFadden B J (Eds) *Magnetite Biomineralization and Magnetoreception in Organisms. A New Biomagnetism* (Topics in Geobiology, Vol. 5) (New York: Plenum Press, 1985) DOI:10.1007/978-1-4613-0313-8
22. Binhi V N, Chernavsky D S *Biophysics* **50** 599 (2005); *Biofizika* **50** 684 (2005)
23. Sokolik I A, Frankevich E L *Sov. Phys. Usp.* **16** 687 (1974); *Usp. Fiz. Nauk* **111** 261 (1973)
24. Brocklehurst B *Nature* **221** 921 (1969)
25. Buchachenko A L, Sagdeev R Z, Salikhov K M *Magnitnye i Spinovye Effekty v Khimicheskikh Reaktsiyakh* (Magnetic and Spin Effects in Chemical Reactions) (Exec. Ed. Yu N Molin) (Novosibirsk: Nauka, 1978); see also: Salikhov K M, Molin Yu N, Sagdeev R Z, Buchachenko A L *Spin Polarization and Magnetic Effects in Radical Reactions* (Studies in Physical and Theoretical Chemistry, Vol. 22, Ed. Yu N Molin) (Amsterdam: Elsevier, 1984)
26. Zel'dovich Ya B, Buchachenko A L, Frankevich E L *Sov. Phys. Usp.* **31** 385 (1988); *Usp. Fiz. Nauk* **155** 3 (1988)
27. Steiner U E, Ulrich T *Chem. Rev.* **89** (1) 51 (1989)
28. Bagryansky V A, Borovkov V I, Molin Yu N *Russ. Chem. Rev.* **76** 493 (2007); *Usp. Khim.* **76** 535 (2007)
29. Hoff A J et al. *Biochim. Biophys. Acta BBA Bioenergetics* **460** 547 (1977)
30. Schulten K, Swenberg C E, Weller A *Z. Phys. Chem. Neue Folge* **111** (1) 1 (1978)
31. Wiltschko R, Wiltschko W *BioEssays* **28** 157 (2006)
32. Maeda K et al. *Nature* **453** 387 (2008)
33. Cai J, Guerreschi G G, Briegel H J *Phys. Rev. Lett.* **104** 220502 (2010)
34. Kominis I K *Chem. Phys. Lett.* **542** 143 (2012)
35. Tiersch M et al. *J. Phys. Chem. A* **118** (1) 13 (2014)
36. Ritz T, Adem S, Schulten K *Biophys. J.* **78** 707 (2000)
37. Lin C, Todo T *Genome Biol.* **6** 220 (2005) DOI:10.1186/gb-2005-6-5-220
38. Astakhova L A et al. *Zh. Obshchei Biologii* **80** (2) 83 (2019)
39. Wong S Y et al. *J. R. Soc. Interface* **18** 20210601 (2021)
40. Xu J et al. *Nature* **594** 535 (2021)
41. Fedele G et al. *PLoS Genet.* **10** e1004804 (2014)
42. Lohmann K J et al. *Nature* **428** 909 (2004)
43. Wu H et al. *Sci. Rep.* **10** 7364 (2020)
44. Wan G et al. *Nature Commun.* **12** 771 (2021)
45. Kattnig D R et al. *Nature Chem.* **8** 384 (2016)
46. Rodgers C T, Hore P J *Proc. Natl. Acad. Sci. USA* **106** 353 (2009)
47. Kerpal C et al. *Nature Commun.* **10** 3707 (2019)
48. Bradlaugh A A et al. *Nature* **615** 111 (2023)
49. Hore P J *eLife* **8** e44179 (2019)
50. Hiscock H G et al. *Biophys. J.* **113** 1475 (2017)
51. Binhi V N *Magnetobiology*: *Underlying Physical Problems* (San Diego, CA: Academic Press, 2002)
52. Cremer-Bartels G, Krause K, Küchle H J *Graefe's Arch. Clin. Exp. Ophthalmol.* **220** (5) 248 (1983)
53. Dhiman S K, Galland P *J. Plant Physiol.* **231** 9 (2018)
54. Fu J-P et al. *Protein Cell* **7** 624 (2016)
55. Binhi V N, Prato F S *PLoS ONE* **12** e0179340 (2017) DOI:10.1371/journal.pone.0179340
56. Magin I M et al. *J. Phys. Chem. A* **109** 7396 (2005)
57. Stovbun S V et al. *Sci. Rep.* **13** 465 (2023)
58. Boxer S G, Chidsey C E D, Roelofs M G *Annu. Rev. Phys. Chem.* **34** 389 (1983)
59. Maeda K et al. *Proc. Natl. Acad. Sci. USA* **109** 4774 (2012)
60. Henbest K B et al. *Proc. Natl. Acad. Sci. USA* **105** 14395 (2008)
61. Beardmore J P, Antill L M, Woodward J R *Angew. Chem. Int. Ed.* **127** 8614 (2015)
62. Golesworthy M J et al. *J. Chem. Phys.* **159** 105102 (2023)
63. Höytö A et al. *Int. J. Rad. Biol.* **93** 646 (2017)

64. Agliassa C et al. *J. Photochem. Photobiol. B* **185** 32 (2018)
65. Pooam M et al. *Planta* **249** 319 (2019)
66. Ren J et al. *Front. Phys.* **10** 995860 (2022)
67. Lambinet V et al. *J. Comp. Physiol. A* **203** 1029 (2017)
68. Wang C X et al. *eNeuro* **6** (2) e0483 (2019) DOI:10.1523/ENEURO.0483-18.2019
69. Mandelstam L I, Tamm I E *Izv. Akad. Nauk SSSR Ser. Fiz.* **9** (1–2) 122 (1945); Mandelstam L, Tamm I *J. Phys. USSR* **9** 249 (1945)
70. Sen D *Curr. Sci. India* **107** 203 (2014)
71. Landau L D, Lifshitz E M *Kvantovaya Mekhanika. Nerelyativistskaya Teoriya* 3rd ed., rev. and enlarged (Moscow: Nauka, 1974); Translated into English: *Quantum Mechanics. Non-Relativistic Theory* (Oxford: Pergamon Press, 1977)
72. Binhi V N, Savin A V *Phys. Usp.* **46** 259 (2003); *Usp. Fiz. Nauk* **173** 265 (2003)
73. Binhi V N *Biofizika* **70** 390 (2025)
74. Menskii M B *Phys. Usp.* **46** 1163 (2003); *Usp. Fiz. Nauk* **173** 1199 (2003)
75. Louisell W H *Quantum Statistical Properties of Radiation* (New York: Wiley, 1990)
76. Blum K *Teoriya Matritsy Plotnosti i Ee Prilozheniya* (Moscow: Mir, 1983); Translated from English: *Density Matrix Theory and Applications* (New York: Plenum Press, 1981)
77. Bertini I, Martini G, Luchinat C, in *Handbook of Electron Spin Resonance. Data Sources, Computer Technology, Relaxation, and ENDOR* (Eds C P Poole (Jr.), H A Farach) (New York: AIP Press, 1994) Ch. IV: Relaxation Data Tabulation
78. Goldfarb D, Stoll S (Eds) *EPR Spectroscopy*: *Fundamentals and Methods* (Hoboken, NJ: John Wiley and Sons, 2018)
79. Liedvogel M et al. *PLoS ONE* **2** (10) e1106 (2007) DOI:10.1371/journal.pone.0001106
80. Valiev K A, Kokin A A *Kvantovye Komp'yutery. Nadezhdy i Real'nost'* (Quantum Computers: Hopes and Reality) (Izhevsk: Regulyarnaya i Khaoticheskaya Dinamika, 2001)
81. Canfield J M, Belford R L, Debrunner P G *Mol. Phys.* **89** 889 (1996)
82. Brocklehurst B, McLauchlan K A *Int. J. Rad. Biol.* **69** (1) 3 (1996)
83. Buchachenko A L, Berdinsky V L, Kuznetsov D A *Biophysics* **51** (3) 489 (2006) DOI:10.1134/S0006350906030249; *Biofizika* **51** (3) 545 (2006)
84. Hore P J *Proc. Natl. Acad. Sci. USA* **109** 1357 (2012)
85. Thoradit T et al. *Front. Plant Sci.* **14** 1266357 (2023)
86. Salikhov K M *Chem. Phys.* **82** (1–2) 145 (1983)
87. Ivanov K L et al. *Mol. Phys.* **100** 1197 (2002)
88. Cintolesi F et al. *Chem. Phys.* **294** 385 (2003)
89. Efimova O, Hore P J *Biophys. J.* **94** 1565 (2008)
90. Solov'yov I A, Chandler D E, Schulten K *Biophys. J.* **92** 2711 (2007)
91. Solov'yov I A, Schulten K *Biophys. J.* **96** 4804 (2009)
92. Ritz T *Procedia Chem.* **3** (1) 262 (2011)
93. Cai J *Phys. Rev. Lett.* **106** 100501 (2011)
94. Jones J A, Hore P J *Chem. Phys. Lett.* **488** (1–3) 90 (2010)
95. Bandyopadhyay J N, Paterek T, Kaszlikowski D *Phys. Rev. Lett.* **109** 110502 (2012)
96. Lee A A et al. *J. R. Soc. Interface* **11** 20131063 (2014)
97. Zhang Y, Berman G P, Kais S *Phys. Rev. E* **90** 042707 (2014)
98. Jain R et al. *Proc. R. Soc. London A* **477** 20200778 (2021) DOI:10.1098/rspa.2020.0778
99. Wong S Y, Benjamin P, Hore P J *Phys. Chem. Chem. Phys.* **25** 975 (2023)
100. Kominis I K *Phys. Rev. E* **80** 056115 (2009)
101. Gauger E M et al. *Phys. Rev. Lett.* **106** 040503 (2011)
102. Lambert N et al. *New J. Phys.* **15** 083024 (2013)
103. Abragam A *Yadernyi Magnetizm* (Moscow: IL, 1963); Translated from English: *The Principles of Nuclear Magnetism* (Oxford: Clarendon Press, 1961)
104. Standley K J, Vaughan R A *Electron Spin Relaxation Phenomena in Solids* (New York: Plenum Press, 1969) DOI:10.1007/978-1-4899-6539-4
105. Lebedev Ya S, Muromtsev V I *EPR i Relaksatsiya Stabilizirovannykh Radikalov* (EPR and Relaxation of Stabilized Radicals) (Moscow: Khimiya, 1972)
106. Weil J A, Bolton J R *Electron Paramagnetic Resonance*: *Elementary Theory and Practical Applications* (Hoboken, NJ: Wiley, 2007)
107. Kowalewski J, Mäler L *Nuclear Spin Relaxation in Liquids*: *Theory, Experiments, and Applications* (New York: Taylor and Francis, 2006)
108. Petasis D T *EPR Spectroscopy* (Berlin: de Gruyter, 2022) DOI:10.1515/9783110417562
109. Hemminga M A, Berliner L J *ESR Spectroscopy in Membrane Biophysics* (Biological Magnetic Resonance, Vol. 27) (New York: Springer, 2007) DOI:10.1007/978-0-387-49367-1
110. Möbius K, Savitsky A *Appl. Magn. Reson.* **54** 207 (2023)
111. Bazhin N M, Salikhov K M *EPR. Relaksatsiya Svobodnykh Radikalov v Zhidkostyakh* (EPR. Relaxation of Free Radicals in Liquids) (Novosibirsk: NGU, 1973)
112. Sato H et al. *Mol. Phys.* **105** 2137 (2007)
113. Klug C S, Feix J B, in *Biomedical EPR* Pt. B *Methodology, Instrumentation, and Dynamics* (Biological Magnetic Resonance, Vol. 24, Eds S R Eaton, G R Eaton, L J Berliner) (New York: Kluwer Acad., Plenum Publ., 2005) p. 269, DOI:10.1007/0-306-48533-8_10
114. Biller J R et al. *J. Magn. Reson.* **236** 47 (2013)
115. Brustolon M, Segre U *Appl. Magn. Reson.* **7** 405 (1994)
116. Mailer C et al. *J. Magn. Reson.* **91** 475 (1991)
117. Borovkov V I, Molin Yu N *Dokl. Phys. Chem.* **396** (4–6) 123 (2004); *Dokl. Ross. Akad. Nauk* **396** 633 (2004) DOI:10.1023/B:DOPC.0000033503.81149.87
118. Kubarev S I, Pshenichnov E A, Shustov A S *Theor. Exp. Chem.* **15** (1) 10 (1979)
119. Brocklehurst B *Chem. Soc. Rev.* **31** 301 (2002)
120. Hedin E M K et al. *J. Biochem. Biophys. Methods* **60** 117 (2004)
121. Commoner B, Heise J J, Townsend J *Proc. Natl. Acad. Sci. USA* **42** 710 (1956)
122. Ivancich A et al. *J. Am. Chem. Soc.* **123** 5050 (2001)
123. Trubitsin B V, Tikhonov A N *J. Magn. Reson.* **163** 257 (2003)
124. Jeschke G *Biochim. Biophys. Acta BBA Bioenergetics* **1707** (1) 91 (2005)
125. Antholine W E, in *Biomedical EPR* Pt. A *Free Radicals, Metals, Medicine and Physiology* (Biological Magnetic Resonance, Vol. 23, Eds S R Eaton, G R Eaton, L J Berliner) (New York: Kluwer Acad., Plenum Publ., 2005) p. 417, DOI:10.1007/0-387-26741-7_14
126. Tikhonov A N et al. *Biochim. Biophys. Acta BBA Bioenergetics* **1777** 285 (2008)
127. Connor H D et al. *J. Am. Chem. Soc.* **130** 6381 (2008)
128. Liu A "Electron paramagnetic resonance (EPR) in enzymology", in *Wiley Encyclopedia of Chemical Biology* (Ed. T P Begley) (New York: John Wiley and Sons, 2008) DOI:10.1002/9780470048672.wecb668
129. Biskup T et al. *Angew. Chem. Int. Edit.* **48** 404 (2009)
130. Schleicher E, Weber S, in *EPR Spectroscopy. Applications in Chemistry and Biology* (Topics in Current Chemistry, Vol. 321, Eds M Drescher, G Jeschke) (Berlin: Springer, 2012) p. 41, DOI:10.1007/128_2011_301
131. Schnegg A et al. *J. Phys. Chem. B* **106** 9454 (2002)
132. Stoner J W et al. *J. Magn. Reson.* **170** (1) 127 (2004)
133. Laguta O et al. *Appl. Phys. Lett.* **120** 120502 (2022)
134. Shushin A I *Chem. Phys. Lett.* **181** (2–3) 274 (1991)
135. Afanasyeva M S et al. *Russ. Chem. Rev.* **76** 599 (2007); *Usp. Khim.* **76** 651 (2007)
136. Hiscock H G et al. *Proc. Natl. Acad. Sci. USA* **113** 4634 (2016)
137. Zadeh-Haghighi H, Rishabh R, Simon C *Front. Phys.* **11** 1026460 (2023)
138. Steiner U E, Wu J Q *Chem. Phys.* **162** (1) 53 (1992)
139. Kattnig D R, Solov'yov I A, Hore P J *Phys. Chem. Chem. Phys.* **18** 12443 (2016)
140. Worster S, Kattnig D R, Hore P J *J. Chem. Phys.* **145** 035104 (2016)
141. Fedin M V et al. *Russ. Chem. Bull.* **55** 1703 (2006); *Izv. Ross. Akad. Nauk Ser. Khim.* (10) 1642 (2006)
142. Breuer H-P, Petruccione F *Teoriya Otkrytykh Kvantovykh Sistem* (Moscow–Izhevsk: RKhD, Inst. Komp'yut. Issled., 2010); Translated from English: *The Theory of Open Quantum Systems* (Oxford: Oxford Univ. Press, 2002)
143. Duglav A V *Spin-reshetochnaya Relaksatsiya Elektronov i Yader v Dielektricheskikh Kristallakh s Paramagnitnymi Primesyami* (Spin-lattice Relaxation of Electrons and Nuclei in Dielectric Crystals with Paramagnetic Impurities) (Kazan: Kazan. Univ., 2018)

144. Aminov L K, Malkin B Z *Dinamika i Kinetika Elektronnykh i Spinovykh Vozbuzhdenii v Paramagnitnykh Kristallakh* (Dynamics and Kinetics of Electron and Spin Excitations in Paramagnetic Crystals) (Kazan: Kazan. Univ., 2008)
145. Redfield A G *IBM J. Res. Dev.* **1** (1) 19 (1957)
146. Brocklehurst B *J. Chem. Soc. Faraday Trans. 2* **72** 1869 (1976)
147. Fedin M V, Purtov P A, Bagryanskaya E G *J. Chem. Phys.* **118** 192 (2003)
148. Walters Z B *Phys. Rev. E* **90** 042710 (2014)
149. Kattnig D R et al. *New J. Phys.* **18** 063007 (2016)
150. Haberkorn R *Mol. Phys.* **32** 1491 (1976)
151. Ivanov K L et al. *J. Phys. Chem. A* **114** 9447 (2010)
152. Buchachenko A L, Vasserman A M *Stabil'nye Radikaly* (Stable Radicals) (Moscow: Khimiya, 1973)
153. Timmel C R et al. *Mol. Phys.* **95** (1) 71 (1998)
154. Cai J, Plenio M B *Phys. Rev. Lett.* **111** 230503 (2013)
155. Xiao D-W et al. *Phys. Rev. Lett.* **124** 128101 (2020)
156. Van Kampen N G *Stochastic Processes in Physics and Chemistry* 3rd ed. (Amsterdam: Elsevier, 2007) DOI:10.1016/B978-0-444-52965-7.X5000-4
157. Binhi V *Phys. Rev. E* **112** 014409 (2025)
158. Torrey H C *Phys. Rev.* **76** 1059 (1949)
159. Hore P J, Mouritsen H *Annu. Rev. Biophys.* **45** (1) 299 (2016)
160. Bagryansky V A, Borovkov V I, Molin Yu N *Dokl. Phys. Chem.* **382** (4–6) 62 (2002); *Dokl. Ross. Akad. Nauk* **382** 794 (2002)
161. Bianco G, Ilieva M, Åkesson S *Biol. Lett.* **15** 20180918 (2019)
162. Feintuch A, Vega S, in *EPR Spectroscopy*: *Fundamentals and Methods* (Eds D Goldfarb, S Stoll) (Chichester: John Wiley and Sons, 2018) p. 143
163. Isserlis L *Biometrica* **12** (1–2) 134 (1918)
164. Wang M C, Uhlenbeck G E *Rev. Mod. Phys.* **17** 323 (1945)
165. Uhlenbeck G E, Ornstein L S *Phys. Rev.* **36** 823 (1930)
166. Coffey W T, Kalmykov Yu P, Waldron J T *The Langevin Equation*: *With Applications to Stochastic Problems in Physics, Chemistry and Electrical Engineering* (World Scientific Series in Contemporary Chemical Physics, Vol. 14) 2nd ed. (Singapore: World Scientific, 2004) DOI:10.1142/5343
167. Akhmanov S A, D'yakov Yu E, Chirkin A S *Statisticheskaya Radiofizika i Optika. Sluchainye Kolebaniya i Volny v Lineinykh Sistemakh* (Statistical Radiophysics and Optics. Random Oscillations and Waves in Linear Systems) (Moscow: Fizmatlit, 2010)
168. Orlando T, Kuprov I, Hiller M *J. Magn. Reson. Open* **10–11** 100040 (2022) DOI:10.1016/j.jmro.2022.100040
169. Binhi V N *Biophysics* **40** 671 (1995); *Biofizika* **40** 677 (1995)
170. Binhi V N *J. Chem. Phys.* **151** 204101 (2019)
171. Berestetskii V B, Lifshitz E M, Pitaevskii L P *Quantum Electrodynamics* (Oxford: Pergamon Press, 1982); Translated from Russian: *Kvantovaya Elektrodinamika* (Moscow: Nauka, 1974)
172. Brocklehurst B *J. Chem. Soc. Faraday Trans. 2* **75** 123 (1979)
173. Scaramozzino D et al. *Int. J. Mol. Sci.* **22** 10501 (2021)
174. Leenders R et al. *Eur. J. Biochem.* **211** (1–2) 37 (1993)
175. Lau J C S et al. *J. R. Soc. Interface* **7** (Suppl. 2) S257 (2010) DOI:10.1098/rsif.2009.0399.focus
176. Palekar D, Shiue M, Lien E J *Pharm. Res.* **13** 1191 (1996)
177. Haynes W M (Ed.-in-Chief), Lide D R, Bruno T J (Associate Eds) *CRC Handbook of Chemistry and Physics* 97th ed. (Boca Raton, FL: CRC Press, 2017) DOI:10.1201/9781315380476
178. Atherton N M *Principles of Electron Spin Resonance* (Chichester: Ellis Horwood, 1993)
179. Fournel A et al. *J. Chem. Phys.* **109** 10905 (1998)
180. Moser C C et al. *Nature* **355** 796 (1992)
181. Harkins T T, Grissom C B *Science* **263** 958 (1994)
182. Kadomtsev B B, Kadomtsev M B *Phys. Usp.* **40** 609 (1996); *Usp. Fiz. Nauk* **166** 651 (1996)
183. Kadomtsev B B *Dinamika i Informatsiya* (Dynamics and Information) (Moscow: Redaktsiya Zhurnala ''Uspekhi Fizicheskikh Nauk'', 1997)
184. Fischer H *Chem. Phys. Lett.* **100** 255 (1983)
185. Hamilton C A et al. *Mol. Phys.* **65** 423 (1988)
186. Saik V O, Ostafin A E, Lipsky S *J. Chem. Phys.* **103** 7347 (1995)
187. Sacher M, Grampp G *Berichte Bunsengesell. phys. Chemie* **101** 971 (1997) DOI:10.1002/bbpc.19971010613
188. Paul S et al. *Sci. Rep.* **7** 11892 (2017)
189. Schulten Z, Schulten K *J. Chem. Phys.* **66** 4616 (1977)
190. Stass D V, Tadjikov B M, Molin Yu N *Chem. Phys. Lett.* **235** (5–6) 511 (1995)
191. Letuta U G et al. *Bioelectromagnetics* **38** 511 (2017)
192. Krylov V et al. *Front. Physiol.* **13** 1040083 (2022)
193. Sinčák M, Sedlakova-Kadukova J *Processes* **11** 282 (2023)
194. Kaspranskii R R, Binhi V N, Koshel' I V *Fiz. Biol. Med.* (1) 77 (2024)
195. Ritz T et al. *Nature* **429** 177 (2004)
196. Engels S et al. *Nature* **509** 353 (2014)
197. Bojarinova J et al. *Sci. Rep.* **10** 3473 (2020)
198. Leberecht B et al. *J. Comp. Physiol. A* **208** 97 (2022)
199. Phillips J, Painter M *Lynx nová série* **53** (1) 219 (2022) DOI:10.37520/lynx.2022.015
200. Kobylkov D et al. *J. R. Soc. Interface* **16** 20190716 (2019)
201. Frankevich E L, Pristupa A I, Lesin V I *Chem. Phys. Lett.* **54** (1) 99 (1978)
202. Lesin V I et al. *Phys. Status Solidi B* **84** 513 (1977)
203. Slichter C P *Principles of Magnetic Resonance* 3rd ed. (Heidelberg: Springer-Verlag, 1996)
204. Kavokin K V *Bioelectromagnetics* **30** 402 (2009)
205. Bargatin I V, Grishanin B A, Zadkov V N *Phys. Usp.* **44** 597 (2001); *Usp. Fiz. Nauk* **171** 625 (2001)
206. Fok V A et al. *Usp. Fiz. Nauk* **16** 436 (1936)
207. Kilin S Ya *Phys. Usp.* **42** 435 (1999); *Usp. Fiz. Nauk* **169** 507 (1999)
208. Kholevo A S *Vvedenie v Kvantovuyu Teoriyu Informatsii* (Introduction to Quantum Information Theory) (Moscow: MTsNMO, 2002)
209. Valiev K A *Phys. Usp.* **48** 1 (2005); *Usp. Fiz. Nauk* **175** 3 (2005)
210. Nielsen M A, Chuang I L *Kvantovye Vychisleniya i Kvantovaya Informatsiya* (Moscow: Mir, 2006); Translated from English: *Quantum Computation and Quantum Information* (Cambridge: Cambridge Univ. Press, 2000)
211. Zheltikov A M, Scully M O *Phys. Usp.* **63** 698 (2020); *Usp. Fiz. Nauk* **190** 749 (2020)
212. Hogben H J, Biskup T, Hore P J *Phys. Rev. Lett.* **109** 220501 (2012)
213. Vesperini A, Bel-Hadj-Aissa G, Franzosi R *Sci. Rep.* **13** 2852 (2023)
214. Horodecki R et al. *Rev. Mod. Phys.* **81** 865 (2009)
215. Eltschka C, Siewert J *J. Phys. A* **47** 424005 (2014)
216. Werner R F *Phys. Rev. A* **40** 4277 (1989)
217. Vedral V et al. *Phys. Rev. Lett.* **78** 2275 (1997)
218. Audretsch J *Entangled Systems. New Directions in Quantum Physics* (Weinheim: Wiley-VCH, 2007) DOI:10.1002/9783527619153
219. Breus T K, Binhi V N, Petrukovich A A *Phys. Usp.* **59** 502 (2016); *Usp. Fiz. Nauk* **186** 568 (2016)
220. Krylov V V et al. *Int. J. Biometeorol.* **63** 241 (2019)
221. Pishchalnikov R Y et al. *Biomed. Signal Proces. Control* **51** 401 (2019)
222. Dorokhov V B et al. *Geofiz. Protsessy Biosfera* **20** (3) 76 (2021) DOI:10.21455/GPB2021.3-5
223. Binhi V N *Cells* **12** 724 (2023)
224. Binhi V N, Rubin A B *Fiz. Biol. Med.* (1) 44 (2023) DOI:10.7256/2730-0560.2023.1.40435
225. Binhi V N, Prato F S *Bioelectromagnetics* **38** (1) 41 (2017)
226. Binhi V N, Savin A V *Phys. Rev. E* **65** 051912 (2002)
227. Bajtoš M et al. *Front. Public Health* **13** 1535155 (2025) DOI:10.3389/fpubh.2025.1535155
228. Binhi V N, Rubin A B *Electromagn. Biol. Med.* **26** (1) 45 (2007)
229. Dhiman S K, Wu F, Galland P *Protoplasma* **260** 767 (2023)
230. Binhi V N, Prato F S *Sci. Rep.* **8** 13495 (2018)
231. Orgel L E *Proc. Natl. Acad. Sci. USA* **67** 1476 (1970)